

Exploiting Higher-Order Statistics for Robust Probabilistic Rounding Error Analysis

Sahil Bhola, Karthik Duraisamy

*Department of Aerospace Engineering & Michigan Institute for Computational Discovery and Engineering,
University of Michigan, Ann Arbor, U.S.A.*

Abstract

Modern computer hardware supports low- and mixed-precision arithmetic for enhanced computational efficiency. In practical predictive modeling, however, it becomes vital to quantify the uncertainty due to rounding along with other sources of uncertainty (such as measurement, sampling, and numerical discretization) to ensure that gain in efficiency does not compromise the model accuracy. Higham and Mary [1] showed that by modeling rounding errors as independent random variables of zero mean, a problem size n dependent constant $\tilde{\gamma}_n \propto \sqrt{n}$ can be obtained that scales slowly compared to the traditional deterministic analysis. In this work, we propose a novel variance-informed probabilistic rounding error analysis by modeling rounding errors as bounded random variables that are independent and identically distributed (i.i.d.). We propose a new problem-size-dependent constant $\hat{\gamma}_n$ that depends on the mean, variance, and the bounds of the rounding error distribution. We show that $\hat{\gamma}_n$ depends on \sqrt{n} , and this functional relation can be obtained rigorously using the statistical information of the rounding errors without making ad-hoc modeling assumptions as in Higham and Mary. This new constant increases gradually with problem size and can improve the rounding error estimates for large arithmetic operations performed at low precision by up to six orders of magnitude. We conduct numerical experiments on random vector dot products, matrix-vector multiplication, a linear system solution, and a stochastic boundary value problem. We show that quantifying rounding uncertainty along with traditional sources (numerical discretization, sampling, parameters) enables a more efficient allocation of computational resources, thereby balancing computational efficiency with predictive accuracy. This study is a step towards a comprehensive mixed-precision approach that improves model reliability and enables budgeting of computational resources in predictive modeling and decision-making.

1. Introduction

In recent years, low-precision arithmetic has gained significant attention in applications such as deep learning [2, 3, 4], climate modeling [5, 6, 7], solution of linear systems of equations [8, 9, 10, 11, 12], fluid dynamics [13, 14, 15], and natural sciences [16]. This is primarily motivated by the lower computational complexity, faster memory access time, a smaller energy footprint, and enhanced data parallelism offered by operating on low-precision numerical data [17, 18, 19, 11, 20, 21]. This strategy for approximate computing is becoming increasingly viable due to advancements in computer architecture (for example, Google’s TPUs and NVIDIA’s GPUs) that provide support for low- or mixed-precision computations for energy efficiency. For example, NVIDIA’s Blackwell architecture supports 4-bit floating-point representation and is estimated to deliver 1.4 exaflops on a single GPU [22]. However, despite the computational advantages, operating on low-precision numerical data introduces significant rounding errors, which can accumulate through successive computations and ultimately impact the accuracy of the computation. This trade-off between computational efficiency and model reliability makes it particularly critical to quantify the uncertainty induced by rounding in conjunction with traditional sources such as measurement, sampling, and numerical discretization [23, 24, 25, 15]. Rigorously quantifying rounding uncertainty alongside traditional sources of uncertainty enables an accurate assessment of computational trade-offs and ensures model integrity where precision is balanced against efficiency.

Traditional deterministic rounding error analysis assumes the worst-case scenario, wherein the absolute rounding errors in every operation are considered to be the unit roundoff u [26, 27, 28, 29,

30, 31]. This approach produces conservative uncertainty estimates and involves the problem-size dependent constant $\gamma_n \triangleq nu/(1 - nu)$, that holds $\forall nu < 1$. Thus, in the regime of large problem sizes and low precision, these bounds fail to produce valid estimates for the rounding uncertainty. For example, even for the dot product of vectors of dimension 10^3 computed in single-precision (`fp32`), the deterministic approach overestimates the rounding uncertainty by $\mathcal{O}(10^2)$ [1].

Several studies have provided a probabilistic description for rounding errors to account for the potential cancellation and magnification of rounding errors to obtain tighter estimates of rounding uncertainty [32, 33, 34, 35, 36]. This has resulted in the heuristic that all problem-size dependent constants in estimating rounding uncertainty can be replaced by their square roots [37, 38]. Recently, pioneering work by Higham and Mary [1] provided a rigorous proof of this widely used criterion by modeling rounding errors as zero-mean independent random variables and thereby introducing a probabilistic problem-size dependent constant $\tilde{\gamma}_n \propto \lambda\sqrt{nu}$ for $\lambda > 0$. Numerical experiments on dot products, matrix-matrix multiplication, and the solution to a dense linear system demonstrated tighter estimates for rounding uncertainty than the deterministic approach. However, the proposed probabilistic error analysis [1, Theorem 2.4] makes an ad-hoc modeling assumption, introducing the \sqrt{n} dependence of $\tilde{\gamma}_n$ as a modeling assumption rather than obtaining it via the random variable treatment of rounding errors. Following [1], Higham and Mary [39] modeled numerical data as independent random variables and considered rounding errors as zero-mean random variables that are mean-independent of all previous numerical data and rounding errors. It was shown that for numerical data distributed with near zero mean, $\tilde{\gamma}_n$ can be relaxed to $\tilde{\gamma}_c \propto cu$ where c is a problem-size independent constant. However, in most practical applications (for example, the solution of linear systems and partial differential equations), numerical data cannot be assumed to be independent as it depends on a previously computed numerical value. More recently, Connolly and Higham [40] showed that tighter probabilistic estimates for rounding uncertainty can be obtained for QR factorization by modeling rounding errors as mean-independent random variables with zero means. Studies thus far have shown that tighter estimates of rounding uncertainty can be obtained by leveraging the statistical description of rounding errors. However, previous studies have only considered the first moment of the rounding errors to develop the probabilistic error analysis.

This work presents a novel probabilistic rounding uncertainty analysis that uses a probabilistic description for rounding errors and can exploit its higher-order statistics. We model rounding errors as bounded, independent, and identically distributed random variables and utilize concentration inequalities that can exploit the mean, variance, and bound information of the rounding errors. Based on the proposed probabilistic analysis (theorem 2.3), our results improve previous probabilistic rounding approaches as follows.

Include higher order-statistics. It provides a general framework wherein the rounding error distribution can be modeled, and the corresponding probabilistic bounds can be obtained by updating the random variable statistics. Unlike previous work that makes assumptions about the rounding error statistics while developing the probabilistic analysis, the proposed approach provides the flexibility to update the underlying rounding error statistics without the probabilistic analysis becoming invalid.

Fewer modeling assumptions. The proposed probabilistic analysis only assumes that the rounding errors are bounded and i.i.d., and can be specialized by making additional assumptions about the distribution of rounding errors. Our analysis provides a rigorous foundation to derive the \sqrt{n} dependence of the problem-size-dependent constant without making unnecessary modeling assumptions about the functional form of the bounds. We show that the \sqrt{n} dependence can be directly obtained using the statistical properties of the rounding error distribution, producing exact bounds without any truncation of higher-order terms. We also demonstrate that the proposed methodology can be applied to the probabilistic approach developed by Higham and Mary [1] to omit unnecessary modeling assumptions. Specifically, we show that the λ parameter in the probabilistic analysis of Higham and Mary [1] can be directly obtained from the bound information of the rounding errors and required confidence in satisfying the probabilistic bounds.

The manuscript is organized as follows. In §2, we present the main result of the paper, the variance-informed probabilistic rounding uncertainty analysis. In §3, we derive the rounding uncertainty estimates for the dot products, matrix-vector multiplication, matrix-matrix multiplication, and the solution of a tri-diagonal system linear system using the Thomas algorithm. Numerical experiments on dot products and matrix-vector multiplication using random data and a stochastic boundary value

problem are presented in §4. The estimates for rounding uncertainty are then systematically compared with other sources of uncertainty, such as numerical discretization and finite sampling. Concluding remarks are presented in §5.

Notation: Scalars are denoted using lowercase letters, for example, a , vectors are denoted using bold lowercase, for example, \mathbf{a} , and matrices are denoted using bold uppercase, for example, \mathbf{A} . Elements of vectors and matrices are denoted using subscripts, that is, $\mathbf{A}_{i,j}$ would be the element in the i^{th} row and j^{th} column. Inequalities established for vectors and matrices hold componentwise, that is, $|\mathbf{A}| \leq |\mathbf{B}|$ means that $|\mathbf{A}_{i,j}| \leq |\mathbf{B}_{i,j}| \forall i, j$. Perturbation to a vector or a matrix is defined componentwise, that is, $\mathbf{A} + \Delta\mathbf{A}$ wherein $\Delta\mathbf{A}$ is the perturbation would mean $\mathbf{A}_{i,j} + \Delta\mathbf{A}_{i,j} \forall i, j$.

2. Bounds for the product of rounding errors

Rounding errors can be interpreted by performing backward and forward error analysis (see Appendix A). In practical applications, bounding backward error via backward error analysis can be advantageous as it can be (a) directly compared with uncertainties in the input and (b) used to derive forward error bounds [28]. These advantages motivate using a backward error analysis approach to estimate rounding uncertainty in this work. Since the backward error implicitly depends upon the rounding operation, we need a model for the underlying rounding operation to obtain backward error estimates and develop useful error bounds. For IEEE standard [41], rounding errors in the case of *no underflow and overflow* can be modeled as

$$fl(z) \triangleq z(1 + \delta)^\rho; \quad z \in \mathbb{R}, \rho = \pm 1, |\delta| \leq u, \quad (1)$$

where δ is the *rounding error* [28]. Here, $\rho = 1$ for the standard computation model and $\rho = -1$ for the alternate computational model.

Performing backward error analysis on numerical algorithms results in the product of terms in the form of $(1 + \delta_i)^{\rho_i}$, where δ_i denotes the rounding error and $\rho_i = \pm 1$ [28]. These terms arise due to the model introduced for rounding operations. For example, consider $y = \sum_{i=1}^3 a_i b_i$ where $a_i, b_i \in \mathbb{R}$. Using eq. (1), the computed approximation \hat{y} to y is given as $\hat{y} = \sum_{i=1}^3 a_i b_i (1 + \xi_i) \prod_{j=\max\{2,i\}}^3 (1 + \kappa_j)$ assuming recursive summation from left to right and no error in representing a_i and b_i in finite-precision. Here, ξ_i, κ_j are the rounding errors, and it is assumed that addition to zero does not introduce any rounding error. In backward error analysis, a bound for $|\prod_{i=1}^n (1 + \delta_i)^{\rho_i} - 1|$ is sought to obtain a perturbed system [28, Chapter 3].

2.1. Deterministic Backward Error Analysis (DBEA)

In the traditional backward error analysis, the following lemma [28, Lemma 3.1] is used to bound the distance between 1 and the product $\prod_{i=1}^n (1 + \delta_i)^{\rho_i}$.

Lemma 2.1 (Deterministic rounding error bound). *If $|\delta_i| \leq u$ and $\rho_i = \pm 1$ for $i = 1, \dots, n$, and $nu < 1$, then*

$$\prod_{i=1}^n (1 + \delta_i)^{\rho_i} = 1 + \theta_n,$$

with $|\theta_n| \leq \gamma_n(u, n) \triangleq \frac{nu}{1-nu}$.

However, this analysis results in conservative estimates for the backward error as it only uses $|\delta_i| \leq u$ and cannot possibly exploit the cancellation of rounding errors [1, 42].

2.2. Mean-informed Backward Error Analysis (MIBEA)

Modeling the rounding errors as random variables has resulted in the heuristic: all constants in the rounding uncertainty analysis that depend on the problem size can be replaced by their square root. Higham and Mary [1] presented a rigorous proof for this criteria and showed that by modeling rounding errors as zero-mean independent random variables, the problem-size dependent constant γ_n in lemma 2.1 can be replaced with

$$\tilde{\gamma}_n(\lambda, u, n) \triangleq \exp\left(\lambda\sqrt{nu} + \frac{nu^2}{1-u}\right) - 1, \quad (2)$$

such that $\prod_{i=1}^n (1 + \delta_i)^{\rho_i} = 1 + \tilde{\theta}_n$ with $|\tilde{\theta}_n| \leq \tilde{\gamma}_n$ with probability at least

$$p_h(\lambda, u) \triangleq 1 - 2 \exp\left(\frac{-\lambda(1-u)^2}{2}\right). \quad (3)$$

Unlike the DBEA, the MIBEA is valid for all problem sizes n and $u < 1$, producing much tighter estimates for a large number of arithmetic operations. *However, in the presented analysis, the \sqrt{n} dependence of $\tilde{\gamma}_n$ was introduced as a modeling assumption rather than obtaining it via the probabilistic treatment of rounding errors. The modeling assumption was motivated only to make the probability bounds independent of the problem size n .* Further, the proposed analysis leveraged Hoeffding's concentration inequality and, therefore, is unable to leverage any available higher-order statistics of rounding errors [43].

2.3. Variance-informed Backward Error Analysis (VIBEA)

We will now introduce a probabilistic rounding uncertainty analysis incorporating higher-order statistics and improving the MIBEA. We assume that the floating point numbers are normalized and there is no underflow or overflow. Similar to [1], the sum of random variables $\sum_{i=1}^n \rho_i \log(1 + \delta_i)$ are bounded by means of a concentration inequality. Specifically, Bernstein's concentration inequality is used to bound the probability that random variable $S_n \triangleq \sum_{i=1}^n Z_i$ deviates from $\mathbb{E}[S_n]$ by a given quantity for a bounded random variable Z_i [43].

Lemma 2.2 (Bernstein's Inequality). *Let Z_1, \dots, Z_n be n independent random variables such that $p(|Z_i| \leq c) = 1$. Then the random variable $S_n \triangleq \sum_{i=1}^n Z_i$ satisfies*

$$p(|S_n - \mathbb{E}[S_n]| \geq t) \leq 2 \exp\left(\frac{-t^2}{2(\sigma^2 + \frac{ct}{3})}\right),$$

$\forall t > 0$, where $\sigma^2 \triangleq \sum_{i=1}^n \text{Var}[Z_i]$.

We can now derive the variance-informed probabilistic backward error bounds leveraging Bernstein's concentration inequality.

Theorem 2.3 (Variance-informed backward error analysis). *Let $\{\delta_i\}_{i=1}^n$ represent n i.i.d. random variables, such that $|\delta_i| \leq u < 1$, where u is the unit roundoff. Then for a required confidence $\zeta \in [0, 1)$,*

$$\prod_{i=1}^n (1 + \delta_i)^{\rho_i} = 1 + \hat{\theta}_n; \quad \rho_i = \pm 1,$$

holds such that $|\hat{\theta}_n| \leq \hat{\gamma}_n(\zeta, u) \triangleq e^{t+n|\mu|} - 1$ with probability at least ζ , where

$$t \triangleq \frac{1}{3} \left(-c \log\left(\frac{1-\zeta}{2}\right) + \sqrt{c^2 \log^2\left(\frac{1-\zeta}{2}\right) - 18n \log\left(\frac{1-\zeta}{2}\right) \sigma^2} \right),$$

$|\log(1 + \delta_i)| \leq c$, $\mu \triangleq \mathbb{E}[\log(1 + \delta_i)]$, and $\sigma^2 \triangleq \text{Var}[\log(1 + \delta_i)]$.

Proof. Define $\log \phi \triangleq \sum_{i=1}^n \rho_i \log(1 + \delta_i)$ as the sum of n i.i.d. random variables $\rho_i \log(1 + \delta_i)$. Let $\mathbb{E}[\log(1 + \delta_i)] \triangleq \mu_i \triangleq \mu$, where the last equality holds under i.i.d. assumption. Similarly, let $\text{Var}[\log(1 + \delta_i)] = \text{Var}[-\log(1 + \delta_i)] \triangleq \sigma_i^2 \triangleq \sigma^2$. Applying lemma 2.2 with $Z_i = \rho_i \log(1 + \delta_i)$

$$p(|\log(\phi) - \mathbb{E}[\log(\phi)]| \geq t) \leq 2 \exp\left(\frac{-t^2}{2(n\sigma^2 + \frac{ct}{3})}\right),$$

$$p(|\log(\phi) - \mathbb{E}[\log(\phi)]| \leq t) \geq 1 - 2 \exp\left(\frac{-t^2}{2(n\sigma^2 + \frac{ct}{3})}\right),$$

where $|\rho_i \log(1 + \delta_i)| = |\log(1 + \delta_i)| \leq c \forall i$. For a required minimum confidence $\zeta \in [0, 1)$ with which $|\log(\phi) - \mathbb{E}[\log(\phi)]| \leq t$ must be satisfied, we can obtain t by solving $t^2 + c_1 t + c_2 = 0$, where $c_1 \triangleq \frac{2c}{3} \log\left(\frac{1-\zeta}{2}\right)$ and $c_2 \triangleq 2n\sigma^2 \log\left(\frac{1-\zeta}{2}\right)$. The roots of this quadratic are given as

$$t_- \triangleq \frac{1}{3} \left(-c \log\left(\frac{1-\zeta}{2}\right) - \sqrt{c^2 \log^2\left(\frac{1-\zeta}{2}\right) - 18n \log\left(\frac{1-\zeta}{2}\right) \sigma^2} \right),$$

$$t_+ \triangleq \frac{1}{3} \left(-c \log\left(\frac{1-\zeta}{2}\right) + \sqrt{c^2 \log^2\left(\frac{1-\zeta}{2}\right) - 18n \log\left(\frac{1-\zeta}{2}\right) \sigma^2} \right),$$

where $t_- < 0$ and $t_+ > 0 \forall n, c, \zeta$, such that $p(|\log(\phi) - \mathbb{E}[\log(\phi)]| \leq t_-) = 0$. Thus, using $t \leftarrow t_+$ and the inequality $|\log(\phi) - \mathbb{E}[\log(\phi)]| \geq |\log(\phi)| - |\mathbb{E}[\log(\phi)]| \geq |\log(\phi)| - n|\mu|$,

$$p(|\log(\phi)| - n|\mu| \leq t_+) \geq p(|\log(\phi) - \mathbb{E}[\log(\phi)]| \leq t_+) \geq \zeta,$$

$$p(|\log(\phi)| \leq t_+ + n|\mu|) \geq \zeta.$$

Thus, $\log(\phi) \in [-(t_+ + n|\mu|), (t_+ + n|\mu|)]$ with probability at least ζ , which gives

$$\phi - 1 \in [e^{-(t_+ + n|\mu|)} - 1, e^{(t_+ + n|\mu|)} - 1].$$

Therefore, we can obtain $|\phi - 1| \leq \max\{|e^{-(t_+ + n|\mu|)} - 1|, |e^{(t_+ + n|\mu|)} - 1|\} = e^{(t_+ + n|\mu|)} - 1 = \hat{\gamma}_n$, which holds with a probability at least ζ . \square

Note that $\hat{\gamma}_{n+1} > \hat{\gamma}_n \forall n$, that is, the bound monotonically increases with the number of arithmetic operations. Theorem 2.3 presents a general framework for performing rounding error analysis while exploiting the statistics of the rounding errors and is valid for all problem sizes n . It is flexible enough that for any distribution of rounding errors δ_i , if the statistics of $\log(1 + \delta_i)$ can be obtained in closed-form, then both mean and variance information can be exploited. Note, compared to the MIBEA presented by Higham and Mary [1], we have not introduced the \sqrt{n} dependence in the error bounds as a modeling assumption, rather rigorously obtained it by exploiting the statistics of the rounding error distribution. By defining a confidence parameter $\zeta \in [0, 1)$ with which the rounding error bounds are satisfied, we can obtain an exact form of the error bounds instead of introducing unnecessary modeling parameters like λ in eq. (2).

This work considers a special case wherein we obtain the rounding error statistics using the following model.

Model 2.4 (Rounding error model). *Rounding error due to finite-precision representation or arithmetic is an i.i.d. random variable distributed uniformly as $\mathcal{U}[-u, u]$.*

Using such a model for rounding error *overpredicts* the rounding error on average, which is desirable for any rounding error analysis since the developed bounds must not bound an under-predicted rounding uncertainty (see Appendix B). Therefore,

$$\mu = \mathbb{E}[\log(1 + \delta_i)] = \frac{-2u + (-1 + u) \log(1 - u) + (1 + u) \log(1 + u)}{2u},$$

$$\sigma^2 = \text{Var}[\log(1 + \delta_i)] = \frac{4u^2 + \kappa[\log^2(1 - u) - 2 \log(1 - u) \log(1 + u) + \log^2(1 + u)]}{4u^2},$$

$$c = \log(1 + u),$$

where $\kappa \triangleq (-1 + u^2)$. Under this special case, we implicitly make the rounding error as zero-mean random variables, unlike the explicit requirement in the MIBEA. Higham and Mary [1] showed that the zero-mean assumption for rounding errors can become invalid, for instance, when adding small positive numbers to large positive numbers. In such cases, the MIBEA fails due to the explicit zero-mean random variable requirement. While the presented results for the VIBEA in this work are specialized using model 2.4, the VIBEA only requires rounding errors to be bounded and i.i.d. Thus, it can be used when the underlying rounding error distribution has a non-zero mean, such as when adding small positive numbers to very large ones. However, modeling the underlying rounding error distribution in such a regime is non-trivial and is not considered in the scope of this study.

2.4. Modified Mean-informed backward error analysis (MMIBEA)

Following the VIBEA, we can also re-derive the MIBEA to omit the ad-hoc modeling assumption that introduces $\lambda\sqrt{n}$ term in $\tilde{\gamma}_n$. We show in theorem 2.6 that while the probabilistic bounds depend on \sqrt{n} , similar to the VIBEA, this dependence can be directly obtained using the statistical properties of the rounding errors.

Lemma 2.5 (Hoeffding's Inequality). *Let Z_1, \dots, Z_n be n independent random variables such that $p(|Z_i| \leq c_i) = 1 \forall i$. Then the random variable $S_n \triangleq \sum_{i=1}^n Z_i$ satisfies*

$$p(|S_n - \mathbb{E}[S_n]| \geq t) \leq 2 \exp\left(\frac{-t^2}{2 \sum_{i=1}^n c_i^2}\right),$$

$\forall t > 0$.

Theorem 2.6 (Modified mean-informed backward error analysis). *Let $\{\delta_i\}_{i=1}^n$ represent n independent zero-mean random variables, such that $|\delta_i| \leq u < 1$, where u is the unit roundoff. Then for a required confidence $\zeta \in [0, 1)$,*

$$\prod_{i=1}^n (1 + \delta_i)^{\rho_i} = 1 + \tilde{\theta}_n; \quad \rho_i = \pm 1,$$

holds such that $|\tilde{\theta}_n| \leq \tilde{\gamma}_n(\zeta, u) \triangleq e^{t + \frac{nu^2}{1-u}} - 1$ with probability at least ζ , where

$$t \triangleq c \sqrt{-2n \log\left(\frac{1-\zeta}{2}\right)},$$

and $|\log(1 + \delta_i)| \leq c = \frac{u}{1-u}$.

Proof. Define $\log \phi \triangleq \sum_{i=1}^n \rho_i \log(1 + \delta_i)$ as the sum of n independent random variables $\rho_i \log(1 + \delta_i)$. For $|\delta_i| \leq u < 1 \forall i$, we can use Taylor series expansion

$$\log(1 + \delta_i) = \sum_{k=1}^{\infty} \frac{(-1)^{k+1} \delta_i^k}{k},$$

to obtain the bounds

$$\begin{aligned} \delta_i - \frac{\delta_i^2}{1 - |\delta_i|} &\leq \log(1 + \delta_i) \leq \delta_i + \frac{\delta_i^2}{1 - |\delta_i|}, \\ \delta_i - \frac{u^2}{1 - u} &\leq \log(1 + \delta_i) \leq \delta_i + \frac{u^2}{1 - u}. \end{aligned}$$

Thus, $|\rho_i \log(1 + \delta_i)| = |\log(1 + \delta_i)| \leq u + \frac{u^2}{1-u} = \frac{u}{1-u} \triangleq c$, and $|\mathbb{E}[\log(1 + \delta_i)]| \leq \frac{u^2}{1-u}$ for $\mathbb{E}[\delta_i] = 0$. Using lemma 2.5 with $Z_i = \rho_i \log(1 + \delta_i)$ and $c_i = c$

$$\begin{aligned} p(|\log(\phi) - \mathbb{E}[\log(\phi)]| \geq t) &\leq 2 \exp\left(\frac{-t^2}{2nc^2}\right), \\ p(|\log(\phi) - \mathbb{E}[\log(\phi)]| \leq t) &\geq 1 - 2 \exp\left(\frac{-t^2}{2nc^2}\right), \end{aligned}$$

For a required minimum confidence $\zeta \in [0, 1)$ with which $|\log(\phi) - \mathbb{E}[\log(\phi)]| \leq t$ must be satisfied, we can obtain t by solving $t^2 + 2nc^2 \log\left(\frac{1-\zeta}{2}\right) = 0$, for which the roots are given as

$$\begin{aligned} t_- &\triangleq -c \sqrt{-2n \log\left(\frac{1-\zeta}{2}\right)}, \\ t_+ &\triangleq c \sqrt{-2n \log\left(\frac{1-\zeta}{2}\right)}, \end{aligned}$$

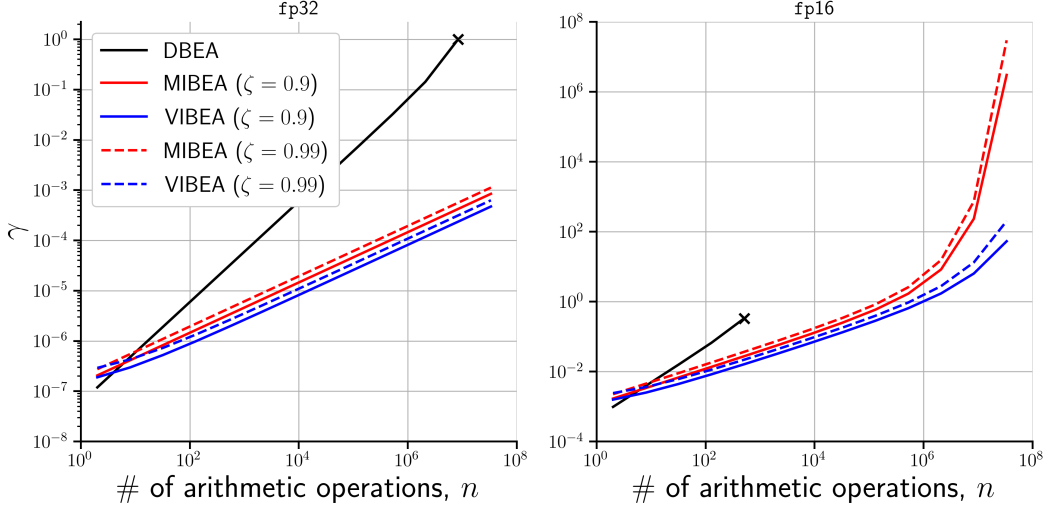


Figure 1: Comparison of the deterministic (DBEA), mean-informed (MIBEA), and variance-informed (VIBEA) probabilistic rounding error bounds with increasing number of arithmetic operations n and varying minimum confidence ζ . For DBEA, the bounds become invalid for large arithmetic operations, as denoted by (X). Across all minimum required confidence, the problem-size dependent constant γ obtained using the VIBEA scale slowly with increasing n and decreasing precision.

where $t_- < 0$ and $t_+ > 0 \forall n, c, \zeta$ such that $p(|\log(\phi) - \mathbb{E}[\log(\phi)]| \leq t_-) = 0$. Thus, using $t \leftarrow t_+$ and the inequality $|\log(\phi) - \mathbb{E}[\log(\phi)]| \geq |\log(\phi) - \mathbb{E}[\log(\phi)]| \geq |\log(\phi) - \frac{nu^2}{1-u}|$,

$$p(|\log(\phi) - \frac{nu^2}{1-u}| \leq t_+) \geq p(|\log(\phi) - \mathbb{E}[\log(\phi)]| \leq t_+) \geq \zeta,$$

$$p(|\log(\phi)| \leq t_+ + \frac{nu^2}{1-u}) \geq \zeta.$$

Thus, $\log(\phi) \in [-t_+ + \frac{nu^2}{1-u}, t_+ + \frac{nu^2}{1-u}]$ with probability at least ζ , which gives

$$\phi - 1 \in [e^{-(t_+ + \frac{nu^2}{1-u})} - 1, e^{(t_+ + \frac{nu^2}{1-u})} - 1].$$

Therefore, we can obtain $|\phi - 1| \leq \max\{|e^{-(t_+ + \frac{nu^2}{1-u})} - 1|, |e^{(t_+ + \frac{nu^2}{1-u})} - 1|\} = e^{(t_+ + \frac{nu^2}{1-u})} - 1 = \tilde{\gamma}_n$, which holds with a probability of at least ζ . \square

Note, compared to modeling assumption $t = \lambda\sqrt{nu} \forall \lambda > 0$ as proposed by Higham and Mary [1], we obtain $t = \frac{u}{1-u} \sqrt{-2n \log\left(\frac{1-\zeta}{2}\right)}$ through statistical properties of the rounding errors. The equivalence holds for $\lambda = \lambda^\dagger \triangleq \frac{1}{1-u} \sqrt{-2 \log\left(\frac{1-\zeta}{2}\right)}$. When choosing $\lambda = \lambda^\dagger$, we can directly compare the MIBEA and VIBEA for any required confidence ζ . Figure 1 illustrates the obtained problem-dependent constant in the case of DBEA (γ_n), MIBEA ($\tilde{\gamma}_n$), and VIBEA ($\hat{\gamma}_n$) with increasing number of arithmetic operations n using **fp32** and **fp16** arithmetic. The problem-size-dependent constant obtained from the VIBEA scales slowly with n compared to the DBEA and MIBEA for all required minimum confidence and precision. Specifically, we note that for low-precision arithmetic (**fp16**, here), the VIBEA-based constant $\hat{\gamma}_n$ can provide $\mathcal{O}(10^6)$ improvement. For a given required confidence ζ , we can then obtain a critical minimum number of arithmetic operations n_c for which $\hat{\gamma}_n < \tilde{\gamma}_n \forall n \geq n_c$, that is, the VIBEA provides tighter bounds compared to the MIBEA. Similarly, we can define the critical minimum number of arithmetic operations n_d for which $\hat{\gamma}_n < \gamma_n \forall n \geq n_d$, that is, the VIBEA provides tighter bounds compared to the DBEA. The critical problem size for **fp32** and **fp16** is tabulated in Table 1. As shown, VIBEA outperforms both the MIBEA and DBEA for small n_c and n_d , which decreases with smaller required confidence.

Table 1: Critical number of arithmetic operations for various confidence levels ζ .

ζ	n_c		n_d	
	fp16	fp32	fp16	fp32
0.5	1	1	2	2
0.90	2	2	4	3
0.95	2	2	5	5
0.99	3	3	8	7
0.999	4	4	11	10

3. Adaption to numerical linear algebra

In this section, we present the VIBEA for (a) dot product of vectors, (b) matrix-vector and matrix-matrix multiplication, and (c) solving a tri-diagonal linear system. These kernels are central to computational science and are foundational to computations such as matrix factorization and solving linear systems of equations via direct or iterative solvers. For example, banded matrices are widely observed in fluid or structural dynamics and control theory applications. Obtaining reliable estimates for the rounding uncertainty can enable the safe use of low-precision arithmetic for large-scale problems. Since in most practical applications, we are interested in accumulated rounding error once the *statistical model is expressed in finite-precision*, here, we consider that the compute and input precision are the same. We show that for all kernels, we can replace the γ_n (via DBEA) or $\tilde{\gamma}_n$ (via MIBEA) with $\hat{\gamma}_n$, as proposed in theorem 2.3.

3.1. Dot products

We first apply theorem 2.3 to compute the dot product of two vectors. We define

$$\mathcal{Q}(\zeta, n) \triangleq 1 - n(1 - \zeta), \quad (4)$$

where $\zeta \in [0, 1)$ is the probability lower bound as defined in theorem 2.3.

Theorem 3.1 (Dot product). *Let $y = \mathbf{a}^T \mathbf{b}$, where $\mathbf{a}, \mathbf{b} \in \mathbb{R}^n$. Under theorem 2.3 and for $\zeta \in [0, 1)$, the computed dot product \hat{y} satisfies*

$$\hat{y} = (\mathbf{a} + \Delta \mathbf{a})^T \mathbf{b} = \mathbf{a}^T (\mathbf{b} + \Delta \mathbf{b}),$$

where $|\Delta \mathbf{a}| \leq \hat{\gamma}_n |\mathbf{a}|$ and $|\Delta \mathbf{b}| \leq \hat{\gamma}_n |\mathbf{b}|$ holds with a probability at least $\mathcal{Q}(\zeta, n)$.

Proof. Assume that the dot product is computed via the recursive relation $s_i = s_{i-1} + a_i b_i$ where $s_0 = 0$, such that the true dot product $y = s_n$. The computed intermediate sum \hat{s}_i can then be represented as

$$\hat{s}_i = (\hat{s}_{i-1} + a_i b_i (1 + \eta_i))(1 + \xi_i); \quad |\eta_i|, |\xi_i| \leq u,$$

where η_i and ξ_i are the rounding error due to multiplication and addition, respectively. Here, $\xi_1 = 0$ since addition to $s_0 = \hat{s}_0 = 0$ does not introduce any rounding error. Therefore, the computed dot product \hat{y} is

$$\begin{aligned} \hat{y} &= \sum_{i=1}^n a_i b_i (1 + \eta_i) \prod_{j=\max\{2, i\}}^n (1 + \xi_j), \\ &= \sum_{i=1}^n a_i b_i (1 + \hat{\theta}_{n-\max\{2, i\}+2}) = \sum_{i=1}^n (a_i + \Delta a_i) b_i = \sum_{i=1}^n a_i (b_i + \Delta b_i), \end{aligned}$$

where $\Delta a_i \triangleq a_i \hat{\theta}_{n-\max\{2, i\}+2}$ and $\Delta b_i \triangleq b_i \hat{\theta}_{n-\max\{2, i\}+2}$. Using theorem 2.3,

$$\begin{aligned} |\Delta a_i| &\leq \hat{\gamma}_{n-\max\{2, i\}+2} |a_i| \leq \hat{\gamma}_n |a_i|, \\ |\Delta b_i| &\leq \hat{\gamma}_{n-\max\{2, i\}+2} |b_i| \leq \hat{\gamma}_n |b_i|, \end{aligned}$$

is satisfied with probability at least ζ and will fail with at most $1 - \zeta$. Therefore, from the principles of inclusion and exclusion of probabilities, the bound for at least one i will fail with probability at most $\sum_{i=1}^n (1 - \zeta) = n(1 - \zeta)$. Thus, the probability that the bounds hold for all i is at least $\mathcal{Q}(\zeta, n)$. \square

To ensure that all the bounds are satisfied, we can set $\mathcal{Q}(\zeta, n)$ to the desired confidence to obtain the probability lower bound for each error bound ζ . Compared to [1], which required the selection of the parameter λ in eq. (2), we can directly construct error bounds with desired confidence. However, as shown in section 2.4, varying λ for a given \mathbf{u} essentially affects the individual bound confidence ζ . Using theorem 3.1, we can also obtain the variance-informed forward error is given as

$$\frac{|\hat{y} - y|}{|y|} \leq \hat{\gamma}_n \frac{|\mathbf{a}^T \mathbf{b}|}{|\mathbf{a}^T \mathbf{b}|}, \quad (5)$$

that holds with probability at least $\mathcal{Q}(\zeta, n)$.

3.2. Matrix-vector and matrix-matrix products

Using theorem 3.1, we can now perform the error analysis for matrix-vector and matrix-matrix multiplications.

Theorem 3.2 (Matrix-vector product). *Let $\mathbf{y} = \mathbf{A}\mathbf{x}$, where $\mathbf{A} \in \mathbb{R}^{m \times n}$, $\mathbf{x} \in \mathbb{R}^n$ and $\mathbf{y} \in \mathbb{R}^m$. Under theorem 2.3 and for $\zeta \in [0, 1)$, the computed matrix-vector product $\hat{\mathbf{y}}$ satisfies*

$$\hat{\mathbf{y}} = (\mathbf{A} + \Delta\mathbf{A})\mathbf{x}; \quad |\Delta\mathbf{A}| \leq \hat{\gamma}_n |\mathbf{A}|,$$

with probability at least $\mathcal{Q}(\zeta, mn)$.

Proof. Let y_i denote the i^{th} element of \mathbf{y} and \mathbf{a}_i denote the i^{th} row of \mathbf{A} . Thus, $y_i = \mathbf{a}_i^T \mathbf{x}$, such that \mathbf{y} can be obtained by performing m dot products of vector size n . Using theorem 3.1, the computed approximation \hat{y}_i to y_i is given as

$$\hat{y}_i = (\mathbf{a}_i + \Delta\mathbf{a}_i)^T \mathbf{x}; \quad |\Delta\mathbf{a}_i| \leq \hat{\gamma}_n |\mathbf{a}_i|,$$

which holds with probability at least $\mathcal{Q}(\zeta, n)$. Since we are performing m dot products, the probability that all the bounds will hold is at least $1 - m(1 - \mathcal{Q}(\zeta, n)) = \mathcal{Q}(\zeta, mn)$. \square

Using theorem 3.2, the variance-informed forward error bound is given as

$$\frac{|\hat{\mathbf{y}} - \mathbf{y}|}{|\mathbf{y}|} \leq \hat{\gamma}_n \frac{|\mathbf{A}||\mathbf{x}|}{|\mathbf{A}\mathbf{x}|}, \quad (6)$$

that holds with probability at least $\mathcal{Q}(\zeta, mn)$. Using theorem 3.2, we can now obtain the error bounds for the matrix-matrix product.

Theorem 3.3 (Matrix-matrix product). *Let $\mathbf{C} = \mathbf{A}\mathbf{B}$, where $\mathbf{A} \in \mathbb{R}^{m \times n}$, $\mathbf{B} \in \mathbb{R}^{n \times t}$ and $\mathbf{C} \in \mathbb{R}^{m \times t}$. Under theorem 2.3 and for $\zeta \in [0, 1)$, the computed approximation $\hat{\mathbf{c}}_j$ of the j^{th} column of \mathbf{C} satisfies*

$$\hat{\mathbf{c}}_j = (\mathbf{A} + \Delta\mathbf{A})\mathbf{b}_j; \quad |\Delta\mathbf{A}| \leq \hat{\gamma}_n |\mathbf{A}| \quad \forall j,$$

with probability at least $\mathcal{Q}(\zeta, mn)$ and

$$\frac{|\hat{\mathbf{C}} - \mathbf{C}|}{|\mathbf{C}|} \leq \hat{\gamma}_n \frac{|\mathbf{A}||\mathbf{B}|}{|\mathbf{A}\mathbf{B}|},$$

is satisfied with probability at least $\mathcal{Q}(\zeta, mnt)$.

Proof. Let \mathbf{c}_j denote the j^{th} column of \mathbf{C} , which can be entirely computed by performing m dot products of vectors of size n . Let \mathbf{b}_j denote the j^{th} column of \mathbf{B} , such that using theorem 3.2

$$\hat{\mathbf{c}}_j = (\mathbf{A} + \Delta\mathbf{A})\mathbf{b}_j; \quad |\Delta\mathbf{A}| \leq \hat{\gamma}_n |\mathbf{A}| \quad \forall j.$$

Thus, $|\hat{\mathbf{c}}_j - \mathbf{c}_j| \leq \hat{\gamma}_n |\mathbf{A}||\mathbf{b}_j| \quad \forall j$ is satisfied with a probability at least $\mathcal{Q}(\zeta, mn)$. Therefore,

$$\frac{|\hat{\mathbf{C}} - \mathbf{C}|}{|\mathbf{C}|} \leq \hat{\gamma}_n \frac{|\mathbf{A}||\mathbf{B}|}{|\mathbf{A}\mathbf{B}|}.$$

The probability that the bounds in the j^{th} column fail is at most $1 - \mathcal{Q}(\zeta, mn)$. Thus, the probability the bounds obtained $\forall j$ are satisfied is at least $1 - t(1 - \mathcal{Q}(\zeta, mn)) = \mathcal{Q}(\zeta, mnt)$. \square

3.3. Thomas algorithm

The Thomas algorithm is widely used to compute the solution of a tri-diagonal system $\mathbf{Ax} = \mathbf{b}$. Broadly, it consists of three steps

1. Compute LU-factorization of \mathbf{A} as $\mathbf{LU} = \mathbf{A}$.
2. Perform forward substitution to solve the system $\mathbf{Ly} = \mathbf{b}$.
3. Perform backward substitution to solve the system $\mathbf{Ux} = \mathbf{y}$.

Computing the solution of the system in finite precision is therefore associated with rounding errors in all three steps. Thus, to determine the backward error bounds on \mathbf{A} , we must first individually determine backward error bounds for each of the outlined steps. First, consider the LU-factorization for which the variance-informed backward error bound is given in lemma 3.4.

Lemma 3.4 (LU decomposition of tri-diagonal system). *Let $\mathbf{A} = \mathbf{LU}$ be the LU-factorization of a tri-diagonal matrix $\mathbf{A} \in \mathbb{R}^{n \times n}$. Under theorem 2.3 and for $\zeta \in [0, 1)$, the computed factorization $\hat{\mathbf{L}} \in \mathbb{R}^{n \times n}$ and $\hat{\mathbf{U}} \in \mathbb{R}^{n \times n}$ via Doolittle's method satisfies*

$$\hat{\mathbf{L}}\hat{\mathbf{U}} = \mathbf{A} + \Delta\mathbf{A},$$

such that $|\Delta\mathbf{A}| \leq \hat{\gamma}_1 |\hat{\mathbf{L}}| |\hat{\mathbf{U}}|$ holds with a probability at least $\mathcal{Q}(\zeta, 3(n-1))$.

Proof. Let $\mathbf{A} \in \mathbb{R}^{n \times n}$ be a tri-diagonal matrix with non-zero elements

$$\mathbf{A}_{i,j} = \begin{cases} \alpha_i & \text{for } j = i - 1 \text{ and } i = 2, \dots, n, \\ \beta_i & \text{for } j = i \text{ and } i = 1, \dots, n, \\ \nu_i & \text{for } j = i + 1 \text{ and } i = 1, \dots, n - 1, \end{cases}$$

with $\alpha_i, \beta_i, \nu_i \in \mathbb{R}$. Let $\mathbf{A} = \mathbf{LU}$ be the LU-factorization where the non-zero elements of the factorization are given as

$$\mathbf{L}_{i,j} = \begin{cases} l_i & \text{for } j = i - 1 \text{ and } i = 2, \dots, n, \\ 1 & \text{for } j = i \text{ and } i = 1, \dots, n, \end{cases}$$

$$\mathbf{U}_{i,j} = \begin{cases} u_i & \text{for } j = i \text{ and } i = 1, \dots, n, \\ \nu_i & \text{for } j = i + 1 \text{ and } i = 1, \dots, n - 1. \end{cases}$$

The non-zero elements can be obtained using a recurrence relation via Doolittle's method as

$$\left. \begin{aligned} l_i &= \alpha_i / u_{i-1}, \\ u_i &= \beta_i - l_i \nu_{i-1}, \end{aligned} \right\} \quad \text{for } i = 2, \dots, n,$$

with $u_1 = \beta_1$, such that for any $i = 2, \dots, n$ the computed elements of the factorization are

$$\hat{l}_i = \alpha_i / \hat{u}_{i-1} (1 + \eta_i); \quad |\eta_i| \leq u,$$

$$\hat{u}_i = (\beta_i - \hat{l}_i \nu_{i-1} (1 + \psi_i)) / (1 + \xi_i); \quad |\psi_i|, |\xi_i| \leq u.$$

Using theorem 2.3

$$\hat{l}_i \hat{u}_{i-1} + \hat{\theta}_1 \hat{l}_i \hat{u}_{i-1} = \alpha_i,$$

$$\hat{u}_i + \hat{l}_i \nu_{i-1} + \hat{\theta}'_1 \hat{u}_i + \hat{\theta}''_1 \hat{l}_i \nu_{i-1} = \beta_i,$$

where $|\hat{\theta}_1|, |\hat{\theta}'_1|, |\hat{\theta}''_1| \leq \hat{\gamma}_1$ is satisfied with probability at least ζ . Thus, via the inclusion-exclusion principle, all the bounds for a given i are satisfied with probability at least $\mathcal{Q}(\zeta, 3)$. In matrix notation, the computed factorization can then be expressed as $\hat{\mathbf{L}}\hat{\mathbf{U}} = \mathbf{A} + \Delta\mathbf{A}$, where $|\Delta\mathbf{A}| \leq \hat{\gamma}_1 |\hat{\mathbf{L}}| |\hat{\mathbf{U}}|$, such that all the bounds are satisfied with a probability at least $1 - \sum_{i=2}^n (1 - \mathcal{Q}(\zeta, 3)) = \mathcal{Q}(\zeta, 3(n-1))$. \square

Next, lemma 3.5 outlines the variance-informed backward error bounds for performing forward substitution in the Thomas algorithm.

Lemma 3.5 (Forward substitution in Thomas Algorithm). *Let $\mathbf{L}\mathbf{y} = \mathbf{b}$ be a tri-diagonal system where $\mathbf{L} \in \mathbb{R}^{n \times n}$ is the lower-triangular matrix obtained from the LU-factorization of a tri-diagonal matrix $\mathbf{A} \in \mathbb{R}^{n \times n}$. Under theorem 2.3 and for $\zeta \in [0, 1)$, the computed solution $\hat{\mathbf{y}}$ via forward substitution satisfies*

$$(\mathbf{L} + \Delta\mathbf{L})\hat{\mathbf{y}} = \mathbf{b},$$

such that $|\Delta\mathbf{L}| \leq \hat{\gamma}_1|\mathbf{L}|$ holds with a probability at least $\mathcal{Q}(\zeta, 2(n-1))$.

Proof. Let $\mathbf{L}\mathbf{y} = \mathbf{b}$ be a triangular system where \mathbf{L} is the lower-triangular matrix obtained from the LU-factorization of a tri-diagonal matrix via Dolittle's decomposition. The non-zero elements of \mathbf{L} are given as

$$\mathbf{L}_{i,j} = \begin{cases} l_i & \text{for } j = i-1 \text{ and } i = 2, \dots, n, \\ 1 & \text{for } j = i \text{ and } i = 1, \dots, n. \end{cases}$$

The system can then be solved via forward substitution as

$$y_i = \begin{cases} b_i & \text{for } i = 1, \\ b_i - l_i y_{i-1} & \text{for } i = 2, \dots, n, \end{cases}$$

such that the computed solution is given as

$$\hat{y}_i = \begin{cases} b_i & \text{for } i = 1, \\ \frac{b_i - l_i \hat{y}_{i-1} (1 + \eta_i)}{(1 + \xi_i)} & \text{for } i = 2, \dots, n, \end{cases}$$

where $|\eta_i|, |\xi_i| \leq u$. Using theorem 2.3,

$$\hat{y}_i + l_i \hat{y}_{i-1} + \hat{\theta}_1 \hat{y}_i + \hat{\theta}'_1 l_i \hat{y}_{i-1} = b_i,$$

where $|\hat{\theta}_1|, |\hat{\theta}'_1| \leq \hat{\gamma}_1$ with probability at least ζ . Thus, for a given i , all the bounds are satisfied with a probability of at least $\mathcal{Q}(\zeta, 2)$. In matrix notation, the computed solution can then be represented as

$$(\mathbf{L} + \Delta\mathbf{L})\hat{\mathbf{y}} = \mathbf{b},$$

where $|\Delta\mathbf{L}| \leq \hat{\gamma}_1|\mathbf{L}|$, such that all the bounds are satisfied with a probability at least $1 - \sum_{i=2}^n (1 - \mathcal{Q}(\zeta, 2)) = \mathcal{Q}(\zeta, 2(n-1))$. \square

Lastly, we can obtain the variance-informed backward error bounds for performing the backward substitution in the Thomas algorithm, as outlined in lemma 3.6.

Lemma 3.6 (Backward substitution in Thomas Algorithm). *Let $\mathbf{U}\mathbf{x} = \mathbf{y}$ be a tri-diagonal system where $\mathbf{U} \in \mathbb{R}^{n \times n}$ is the upper-triangular matrix obtained from the LU-factorization of a tri-diagonal matrix $\mathbf{A} \in \mathbb{R}^{n \times n}$. Under theorem 2.3 and for $\zeta \in [0, 1)$, the computed solution $\hat{\mathbf{x}}$ via backward substitution satisfies*

$$(\mathbf{U} + \Delta\mathbf{U})\hat{\mathbf{x}} = \mathbf{y},$$

such that $|\Delta\mathbf{U}| \leq \hat{\gamma}_2|\mathbf{U}|$ holds with a probability at least $\mathcal{Q}(\zeta, 2n-1)$.

Proof. Let $\mathbf{U}\mathbf{x} = \mathbf{y}$ be a triangular system where \mathbf{U} is the upper triangular matrix obtained from the LU-factorization of a tri-diagonal matrix via Dolittle's decomposition. The non-zero elements of \mathbf{U} are given as

$$\mathbf{U}_{i,j} = \begin{cases} u_i & \text{for } j = i \text{ and } i = 1, \dots, n, \\ \nu_i & \text{for } j = i+1 \text{ and } i = 1, \dots, n-1. \end{cases}$$

The system can then be solved via backward substitution as

$$x_i = \begin{cases} \frac{y_n}{u_n} & \text{for } i = n, \\ \frac{y_i - \nu_i x_{i+1}}{u_i} & \text{for } i = n-1, \dots, 1, \end{cases}$$

such that the computed solution is given as

$$\hat{x}_i = \begin{cases} \frac{y_n}{u_n(1+\eta_i)} & \text{for } i = n, \\ \frac{y_i - \nu_i \hat{x}_{i+1} (1 + \psi_i)}{u_i(1+\xi_i)(1+\chi_i)} & \text{for } i = n-1, \dots, 1, \end{cases}$$

where $|\eta_i|, |\psi_i|, |\xi_i|, |\chi_i| \leq u$. Using theorem 2.3

$$\begin{aligned} \hat{x}_n u_n + \hat{\theta}_1 \hat{x}_n u_n &= y_n, \\ u_i \hat{x}_i + \nu_i \hat{x}_{i+1} + \hat{\theta}_2 u_i \hat{x}_i + \hat{\theta}'_1 \nu_i \hat{x}_{i+1} &= y_i; \quad \text{for } i = n-1, \dots, 1, \end{aligned}$$

where $|\hat{\theta}_1|, |\hat{\theta}'_1| \leq \hat{\gamma}_1 \leq \hat{\gamma}_2$ with probability at least ζ . Similarly, $|\hat{\theta}_2| \leq \hat{\gamma}_2$ with probability at least ζ . Thus, for a given $i = n-1, \dots, 1$, all the bounds are satisfied with a probability at least $1 - 2(1 - \mathcal{Q}(\zeta, 1)) = \mathcal{Q}(\zeta, 2)$. In matrix notation, the computed solution can then be represented as

$$(\mathbf{U} + \Delta\mathbf{U})\hat{\mathbf{x}} = \mathbf{y},$$

where $|\Delta\mathbf{U}| \leq \hat{\gamma}_2|\mathbf{U}|$, such that all the bounds are satisfied with probability at least

$$1 - \left[\left(\sum_{i=2}^n (1 - \mathcal{Q}(\zeta, 2)) \right) + (1 - \mathcal{Q}(\zeta, 1)) \right] = \mathcal{Q}(\zeta, 2n-1).$$

□

Using lemmas 3.4 to 3.6, we can now obtain the variance-informed backward error bounds for solving a tri-diagonal system of equations.

Theorem 3.7 (Thomas Algorithm). *Let $\mathbf{Ax} = \mathbf{b}$ be a tri-diagonal system with $\mathbf{A} \in \mathbb{R}^{n \times n}$, $\mathbf{x} \in \mathbb{R}^n$ and $\mathbf{b} \in \mathbb{R}^n$. Assume that $\hat{\mathbf{L}}$ and $\hat{\mathbf{U}}$ are the computed LU-factorization of the matrix \mathbf{A} via Doolittle's decomposition. Under theorem 2.3 and for $\zeta \in [0, 1)$, the computed solution $\hat{\mathbf{x}}$ satisfies*

$$(\mathbf{A} + \Delta\mathbf{A})\hat{\mathbf{x}} = \mathbf{b},$$

where $|\Delta\mathbf{A}| \leq \hat{\gamma}_{LS}|\hat{\mathbf{L}}||\hat{\mathbf{U}}|$ holds with a probability at least $\mathcal{Q}(\zeta, 7n-6)$ and $\hat{\gamma}_{LS} \triangleq (2\hat{\gamma}_1 + \hat{\gamma}_2 + \hat{\gamma}_1\hat{\gamma}_2)$.

Proof. From lemma 3.4, the computed LU-factorization $\hat{\mathbf{L}}$ and $\hat{\mathbf{U}}$ satisfies $\hat{\mathbf{L}}\hat{\mathbf{U}} = (\mathbf{A} + \Delta\mathbf{A}')$ where component-wise $|\Delta\mathbf{A}'| \leq \hat{\gamma}_1|\hat{\mathbf{L}}||\hat{\mathbf{U}}|$ holds with probability at least $\mathcal{Q}(\zeta, 3(n-1))$. By lemma 3.5, forward substitution results in a computed solution $\hat{\mathbf{y}}$ which satisfies

$$(\hat{\mathbf{L}} + \Delta\hat{\mathbf{L}})\hat{\mathbf{y}} = \mathbf{b},$$

where component-wise $|\Delta\hat{\mathbf{L}}| \leq \hat{\gamma}_1|\hat{\mathbf{L}}|$ is satisfied with probability at least $\mathcal{Q}(\zeta, 2(n-1))$. For backward substitution, via lemma 3.6, the computed solution $\hat{\mathbf{x}}$ satisfies

$$(\hat{\mathbf{U}} + \Delta\hat{\mathbf{U}})\hat{\mathbf{x}} = \hat{\mathbf{y}},$$

where component-wise $|\Delta\hat{\mathbf{U}}| \leq \hat{\gamma}_2|\hat{\mathbf{U}}|$ is satisfied with probability at least $\mathcal{Q}(\zeta, 2n-1)$. Thus,

$$\begin{aligned} (\hat{\mathbf{L}} + \Delta\hat{\mathbf{L}})(\hat{\mathbf{U}} + \Delta\hat{\mathbf{U}})\hat{\mathbf{x}} &= \mathbf{b}, \\ (\mathbf{A} + \Delta\mathbf{A}' + \hat{\mathbf{L}}\Delta\hat{\mathbf{U}} + \Delta\hat{\mathbf{L}}\hat{\mathbf{U}} + \Delta\hat{\mathbf{L}}\Delta\hat{\mathbf{U}})\hat{\mathbf{x}} &= \mathbf{b}, \\ (\mathbf{A} + \Delta\mathbf{A})\hat{\mathbf{x}} &= \mathbf{b}, \end{aligned}$$

where $\Delta\mathbf{A} \triangleq \Delta\mathbf{A}' + \hat{\mathbf{L}}\Delta\hat{\mathbf{U}} + \Delta\hat{\mathbf{L}}\hat{\mathbf{U}} + \Delta\hat{\mathbf{L}}\Delta\hat{\mathbf{U}}$ and $|\Delta\mathbf{A}| \leq (2\hat{\gamma}_1 + \hat{\gamma}_2 + \hat{\gamma}_1\hat{\gamma}_2)|\hat{\mathbf{L}}||\hat{\mathbf{U}}|$ is satisfied with probability at least

$$1 - [(1 - \mathcal{Q}(\zeta, 3(n-1))) + (1 - \mathcal{Q}(\zeta, 2(n-1)))] + (1 - \mathcal{Q}(\zeta, 2n-1)) = \mathcal{Q}(\zeta, 7n-6).$$

□

4. Numerical experiments

This section presents numerical experiments to study the performance of the VIBEA compared to DBEA and MIBEA. First, the variance-informed rounding uncertainty analysis is conducted for the dot product of random vectors. Following this, we study matrix-matrix multiplication, where matrices are sampled randomly. Lastly, we examine a stochastic boundary-value problem with underlying uncertainties due to parameters, numerical discretization, sampling, and rounding. Such statistical models are widely used in practice wherein different sources of uncertainties must be quantified for optimal computational resource allocation while ensuring reliable model predictions. In addition to studying the tightness of different rounding error analysis methodologies, we also study the performance of model 2.4 to ensure that the uniform distribution assumption of random errors does, in fact produce similar accumulated rounding errors as observed in practice. This is necessary to ensure that any probabilistic error bounds leveraging model 2.4 are not bounding an under-predicted rounding error. All numerical experiments are performed using C++ with CUDA 12.5 libraries on an A100 GPU, where the ‘exact’ or ‘ground truth’ values are computed using fp64.

4.1. Dot product of random vectors

Consider a dot product of random vectors $\mathbf{a}, \mathbf{b} \in \mathbb{R}^n$ given as $y = \mathbf{a}^T \mathbf{b}$. Numerically, this dot product is computed using the recursive relation $s_i = s_{i-1} + a_i b_i$ with $s_0 = 0$, such that $y = s_n$. Theoretically, the backward error for the computed dot product \hat{y} is given as

$$\epsilon_{bwd} = \min\{\epsilon \geq 0 : \hat{y} = (\mathbf{a} + \Delta \mathbf{a})^T \mathbf{b}, |\Delta \mathbf{a}| \leq \epsilon |\mathbf{a}|\} = \frac{|\hat{y} - y|}{|\mathbf{a}^T \mathbf{b}|}, \quad (7)$$

which is a random variable in the case where \mathbf{a} and \mathbf{b} are random vectors [28]. Figure 2 illustrates

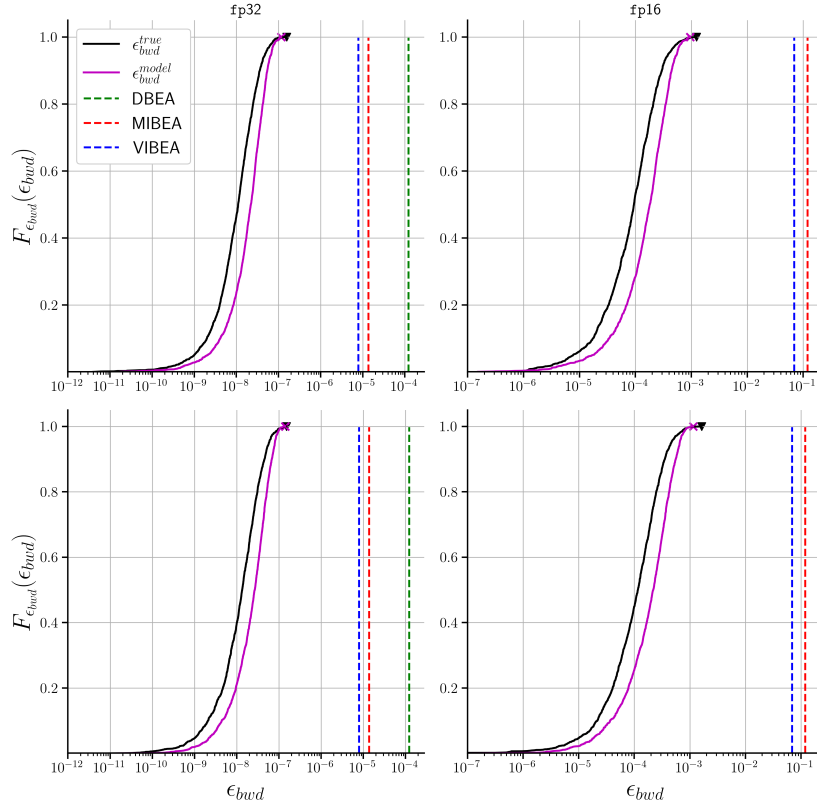


Figure 2: Empirical distribution function of the true backward error, modeled backward error (model 2.4), and its bounds for the dot product of random vectors of size $n = 2^{11}$ distributed as $\mathcal{U}[-1, 1]$ (top row) and $\mathcal{N}(0, 1)$ (bottom row). Here, to obtain the statistics, 10^4 independent experiments were conducted, and to obtain the error bounds $\mathcal{Q}(\zeta, n) = 0.99$. Largest true backward error (\blacktriangledown) is similar to the modeled backward error (\times). For DBEA, the bounds become invalid for low precision arithmetic fp16. VIBEA produces tighter estimates of the backward error compared to DBEA and MIBEA.

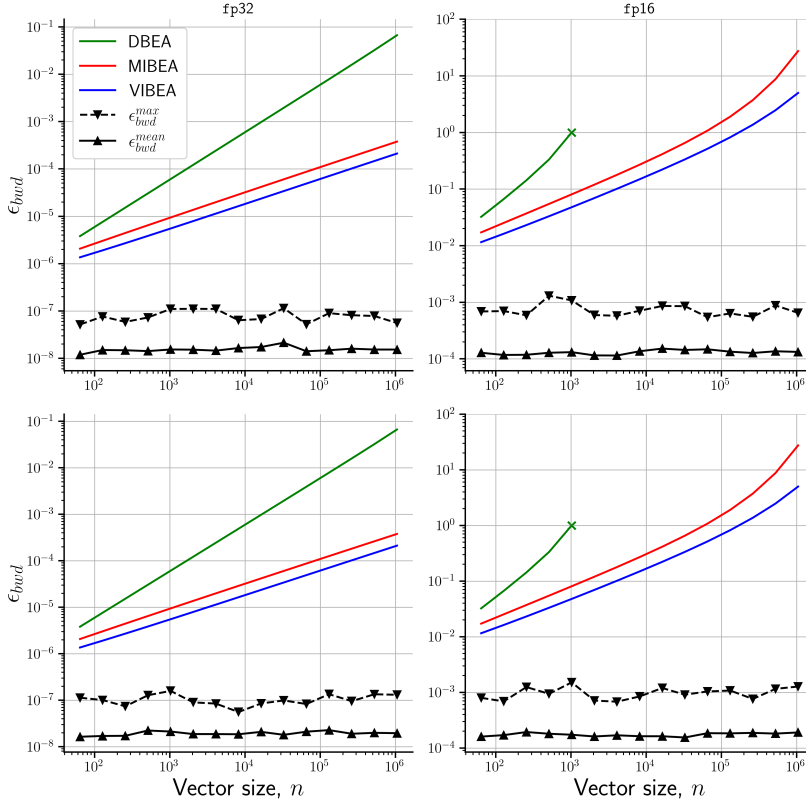


Figure 3: Backward error and its bounds for the dot product of random vectors distributed as $\mathcal{U}[-1, 1]$ (top row) and $\mathcal{N}(0, 1)$ (bottom row). Here, to obtain the statistics, 10^2 independent experiments were conducted, and to obtain the error bounds $\mathcal{Q}(\zeta, n) = 0.99$. For DBEA, the bounds become invalid for large arithmetic operations, as denoted by (X).

the empirical distribution function (EDF) of the true backward error, modeled backward error (using model 2.4), and the obtained bounds for $n = 2^{11}$. For a random variables X , the EDF is defined as $F_X(t) \triangleq \frac{1}{n} \sum_{i=1}^n \mathbf{1}_{X=x_i \leq t} \in [0, 1]$, where x_i denotes an observation of the random variable X and $\mathbf{1}$ is an indicator function. Thus, if $F_{X_1}(t) < F_{X_2}(t)$, where X_1 and X_2 are random variables defined on the same support, would mean that there is a *smaller probability* that X_1 is less than t compared to X_2 . We examine the backward error EDF where $\mathbf{a}, \mathbf{b} \sim \mathcal{U}[-1, 1]$ and $\mathbf{a}, \mathbf{b} \sim \mathcal{N}(0, 1)$ and computations are performed using **fp32** and **fp16** arithmetic. For both the cases, the modeled backward error ϵ_{bwd}^{model} EDF lower bounds the true backward error ϵ_{bwd}^{true} , that is on average, using model 2.4 *overestimates* the true backward error. This is desirable since any bounds developed using model 2.4 must not bound an under-predicted backward error. For all cases, the error bounds obtained using the VIBEA are tighter than those obtained using the MIBEA and DBEA. Note, despite the use of model 2.4 that implicitly results in zero-mean rounding errors (similar to the MIBEA), using higher-order statistics information improves the bounds. Further, as expected, for a large number of arithmetic operations performed at lower precision, the DBEA becomes invalid as nu becomes greater than 1.

Figure 3 illustrates the backward error and its bounds obtained using the deterministic and probabilistic analysis for dot products of random vectors of size n . We conduct two experiments: $\mathbf{a}, \mathbf{b} \sim \mathcal{U}[-1, 1]$ and $\mathbf{a}, \mathbf{b} \sim \mathcal{N}(0, 1)$. For both cases, we observe that the backward error stays nearly constant. Compared to DBEA and MIBEA, the variance-informed probabilistic bounds produce tighter estimates and scale well with problem size. For low-precision arithmetic (**fp16**, here), error bounds based on the MIBEA grow more rapidly for large arithmetic operations, becoming increasingly unreliable. For large arithmetic operations using **fp16**, VIBEA produces nearly an order of magnitude improvement in the error bounds compared to the MIBEA.

4.2. Matrix-vector product

We now consider the Matrix-vector product $\mathbf{y} = \mathbf{A}\mathbf{x}$, where $\mathbf{A} \in \mathbb{R}^{n \times n}$ and $\mathbf{x} \in \mathbb{R}^n$ are sampled from an underlying distribution. Theoretically, the backward error can be obtained using the Oettli-

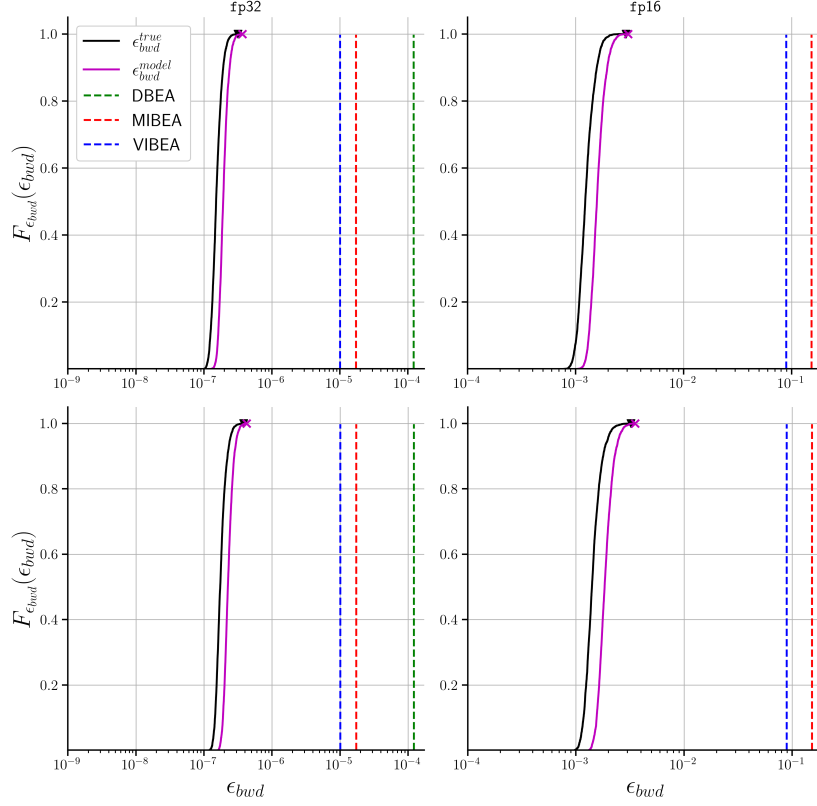


Figure 4: Empirical distribution function of the true backward error, modeled backward error (model 2.4), and its bounds for Matrix-vector product $\mathbf{A}\mathbf{x}$, with $\mathbf{A} \in \mathbb{R}^{n \times n}$ and $\mathbf{x} \in \mathbb{R}^n$ with random entries distributed as $\mathcal{U}[-1, 1]$ (top row) and $\mathcal{N}(0, 1)$ (bottom row) for $n = 2^{11}$. Here, 10^4 independent experiments were conducted to obtain the statistics and get the error bounds $\mathcal{Q}(\zeta, n^2) = 0.99$. Largest true backward error (\blacktriangledown) is similar to the largest modeled backward error (\times). For DBEA, the bounds become invalid for low precision arithmetic **fp16**. VIBEA produces tighter estimates of the backward error compared to DBEA and MIBEA.

Prager theorem [44, 28]

$$\epsilon_{bwd} = \min\{\epsilon \geq 0 : \hat{\mathbf{y}} = (\mathbf{A} + \Delta\mathbf{A})\mathbf{x}, |\Delta\mathbf{A}| \leq \epsilon|\mathbf{A}|\} = \max_i \frac{|\hat{\mathbf{y}} - \mathbf{y}|_i}{(|\mathbf{A}||\mathbf{x}|)_i}, \quad (8)$$

which is a random variable when \mathbf{A} and \mathbf{x} are random. We consider two cases, first where entries of \mathbf{A} and \mathbf{x} are sampled via $\mathcal{U}[-1, 1]$, and second where the underlying distribution is $\mathcal{N}(0, 1)$. Figure 4 shows the EDF of the true backward error, modeled backward error, and its bounds for the matrix-vector product for $n = 2^{11}$. For both cases, we notice that the modeled backward error ϵ_{bwd}^{model} marginally overestimates the true backward error and, therefore, can be used to develop the probabilistic bounds. As shown, VIBEA-based error bounds produce tighter estimates than those obtained using the MIBEA or DIBEA. Further, as shown in fig. 5, the obtained bounds scale well with matrix size and, therefore, can be used to obtain reliable rounding error estimates for large problems.

4.3. Stochastic boundary value problem

Consider the following boundary-value ordinary differential equation (ODE) with random coefficients and random forcing (adapted from [45])

$$\frac{d}{dx} \left((1 + \theta_1 x) \frac{du}{dx} \right) = -50\theta_2^2; \quad x \in [0, 1]; \quad u(0) = u(1) = 0, \quad (9)$$

where $\theta_1 \sim \mathcal{U}[0, 1] + 0.1$ and $\theta_2 \sim \mathcal{U}[0, 1] + 1$. The quantity of interest is $q = \mathbb{E}[P]$, where a realization of the variable P is given as

$$p(\theta_1, \theta_2) = \int_x u dx = \frac{25\theta_2^2(-2\theta_1 + (2 + \theta_1) \log(1 + \theta_1))}{\theta_1^2 \log(1 + \theta_1)}.$$

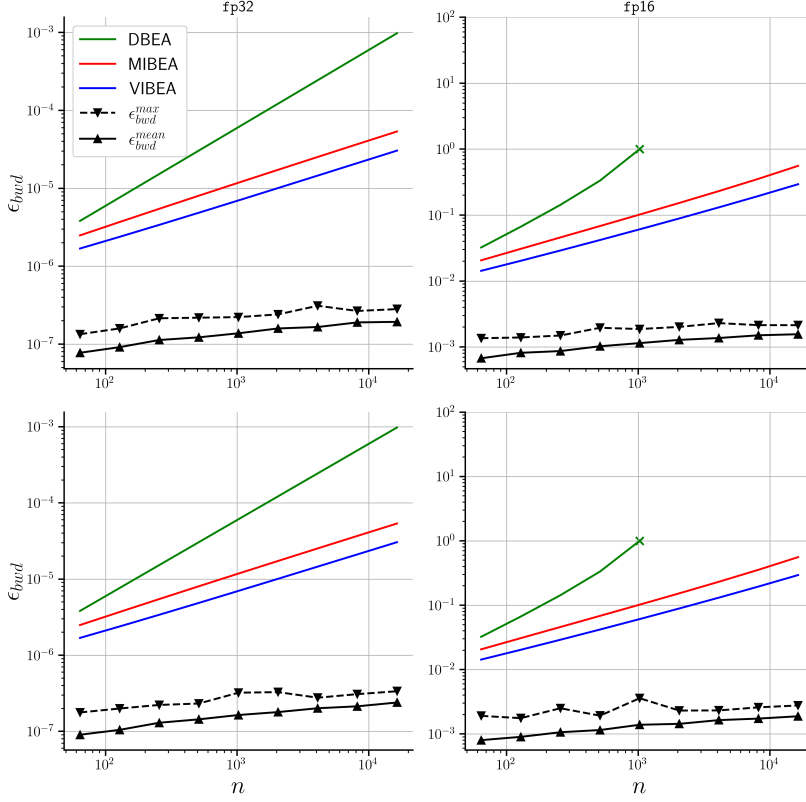


Figure 5: Backward error and its bounds for Matrix-vector product $\mathbf{A}\mathbf{x}$, with $\mathbf{A} \in \mathbb{R}^{n \times n}$ and $\mathbf{b} \in \mathbb{R}^n$ with random entries distributed as $\mathcal{U}[-1, 1]$ (top row) and $\mathcal{N}(0, 1)$ (bottom row). Here, 10^2 independent experiments were conducted to obtain the statistics and to obtain the error bounds $\mathcal{Q}(\zeta, n^2) = 0.99$. For DBEA, the bounds become invalid for large arithmetic operations, as denoted by (\times).

Numerically computing the quantity of interest is associated with multiple sources of uncertainty, namely, (a) parameter uncertainty, (b) numerical discretization, (c) Monte-Carlo integration, and (d) rounding.

4.3.1. Numerical discretization

For a given θ_1, θ_2 , eq. (9) can be discretized via finite-difference method using M intervals of size $\Delta x \triangleq \frac{1}{M}$. Using second-order central difference approximation for the first- and second-order derivatives, the discretized form of the ODE is given as

$$\left(1 + \frac{\theta_1}{M}\left(i - \frac{1}{2}\right)\right)\tilde{u}_{i-1} - 2\left(1 + \frac{\theta_1}{M}i\right)\tilde{u}_i + \left(1 + \frac{\theta_1}{M}\left(i + \frac{1}{2}\right)\right)\tilde{u}_{i+1} = -50\theta_2^2\Delta x^2, \quad (10)$$

where \tilde{u}_i is the discrete solution of $u(x)$ at $x = i\Delta x$ for $i = 1, \dots, M-1$. This results in a tri-diagonal system

$$\mathbf{A}(\theta_1)\tilde{\mathbf{u}} = \mathbf{b}(\theta_2), \quad (11)$$

where $\mathbf{A} \in \mathbb{R}^{(M-1) \times (M-1)}$, $\tilde{\mathbf{u}} \in \mathbb{R}^{(M-1)}$, $\mathbf{b} \in \mathbb{R}^{(M-1)}$. The non-zero elements of \mathbf{A} are given as

$$\begin{aligned} \mathbf{A}_{i,i-1} &\triangleq \alpha_i = 1 + \frac{\theta_1}{M}\left(i - \frac{1}{2}\right) \quad \text{for } i = 2, \dots, M-1, \\ \mathbf{A}_{i,i} &\triangleq \beta_i = -2 - 2\frac{\theta_1}{M}i \quad \text{for } i = 1, \dots, M-1, \\ \mathbf{A}_{i,i+1} &\triangleq \nu_i = 1 + \frac{\theta_1}{M}\left(i + \frac{1}{2}\right) \quad \text{for } i = 1, \dots, M-2. \end{aligned}$$

This system of equations can be solved via the Thomas algorithm to obtain the solution $\tilde{\mathbf{u}}$. Thereafter, an approximation of the integral quantity p given by \tilde{p} can be obtained via Reimann integration as $\tilde{p} = \sum_{i=1}^{M-1} \tilde{u}_i \Delta x$. The approximate quantity of interest \tilde{q} can then be obtained via Monte-Carlo integration.

4.3.2. Discretization error

Solving the ODE in eq. (9) via numerical discretization introduces errors due to (a) coarse discretization (small M) and (b) numerically approximating the spatial derivatives (Taylor series approximation). Herein, we present error bounds due to numerical discretization for a given finite-difference stencil.

For a given θ_1, θ_2 , consider $u(x) = f(x; \theta_1, \theta_2)$ as the ‘true’ solution to the ODE in eq. (9), where $f(x; \theta_1, \theta_2)$ is assumed to be infinitely differentiable. Consider a restrictive operator $\mathcal{R} : \Omega \rightarrow \mathbb{R}^{M-1}$, which maps the true solution from the continuous domain Ω to the discrete space. The error due to numerical approximation is then given as

$$\begin{aligned}\epsilon_d &\triangleq \mathcal{R}u - \tilde{\mathbf{u}}, \\ &= \mathbf{A}^{-1} \mathbf{A} \mathcal{R}u - \mathbf{A}^{-1} \mathbf{b}, \\ &= \mathbf{A}^{-1} (\mathbf{A} \mathcal{R}u - \mathbf{b}).\end{aligned}$$

For the discretized system in eq. (10)

$$(\mathbf{A} \mathcal{R}u - \mathbf{b})_i \triangleq t_i = \alpha_i u_{i-1} + \beta_i u_i + \nu_i u_{i+1} + 50\theta_2^2 \Delta x^2,$$

where $u_i = u(x_i) = f(i\Delta x; \theta_1, \theta_2)$. Using Taylor-series expansion with the Lagrange remainder theorem to represent $u_{i\pm 1}$ gives

$$\begin{aligned}u(x_{i-1}) &= u(x_i) - \Delta x u'(x_i) + \frac{\Delta x^2}{2!} u''(x_i) - \frac{\Delta x^3}{3!} u'''(c_i^-), \\ u(x_{i+1}) &= u(x_i) + \Delta x u'(x_i) + \frac{\Delta x^2}{2!} u''(x_i) + \frac{\Delta x^3}{3!} u'''(c_i^+),\end{aligned}$$

for $c_i^- \in [x_{i-1}, x_i]$ and $c_i^+ \in [x_i, x_{i+1}]$. Since c_i^- and c_i^+ are unknown, we can bound $u(x_{i-1})$ and $u(x_{i+1})$ by defining

$$\begin{aligned}u_{i-1}^{\sup} &\triangleq \sup\{u(x_i) - \Delta x u'(x_i) + \frac{\Delta x^2}{2!} u''(x_i) - \frac{\Delta x^3}{3!} u'''(c_i^-)\}, \\ u_{i-1}^{\inf} &\triangleq \inf\{u(x_i) - \Delta x u'(x_i) + \frac{\Delta x^2}{2!} u''(x_i) - \frac{\Delta x^3}{3!} u'''(c_i^-)\}, \\ u_{i+1}^{\sup} &\triangleq \sup\{u(x_i) + \Delta x u'(x_i) + \frac{\Delta x^2}{2!} u''(x_i) + \frac{\Delta x^3}{3!} u'''(c_i^+)\}, \\ u_{i+1}^{\inf} &\triangleq \inf\{u(x_i) + \Delta x u'(x_i) + \frac{\Delta x^2}{2!} u''(x_i) + \frac{\Delta x^3}{3!} u'''(c_i^+)\},\end{aligned}$$

such that we can obtain the bounds for

$$t_i^{\sup} \triangleq \sup\{\alpha_i * \ell_1 + \beta_i u_i + \nu_i \ell_2 + 50\theta_2^2 \Delta x^3 : \ell_1 \in [u_{i-1}^{\inf}, u_{i-1}^{\sup}], \ell_2 \in [u_{i+1}^{\inf}, u_{i+1}^{\sup}]\}, \quad (12a)$$

$$t_i^{\inf} \triangleq \inf\{\alpha_i * \ell_1 + \beta_i u_i + \nu_i \ell_2 + 50\theta_2^2 \Delta x^3 : \ell_1 \in [u_{i-1}^{\inf}, u_{i-1}^{\sup}], \ell_2 \in [u_{i+1}^{\inf}, u_{i+1}^{\sup}]\}, \quad (12b)$$

which gives $\epsilon_d \in [\mathbf{A}^{-1} \mathbf{t}^{\sup}, \mathbf{A}^{-1} \mathbf{t}^{\inf}]$. Figure 6 illustrates the EDF for the numerical discretization error and its bounds with varying intervals M . As expected, refining the discretization reduces the error introduced due to numerical discretization. Further, the obtained bounds follow the same trend and can predict the numerical discretization error within an order of magnitude.

4.3.3. Rounding error

Computing the finite-precision approximation \hat{p} to the integral quantity \tilde{p} results in several rounding errors. Broadly, rounding errors accumulate when (a) solving the tri-diagonal system as described in §4.3.1, and (b) performing Reimann integration.

For the discretized system given in eq. (11), the theoretical backward error is given as

$$\epsilon_{bwd} = \min\{\epsilon \geq 0 : (\mathbf{A} + \Delta \mathbf{A}) \hat{\tilde{\mathbf{u}}} = \mathbf{b}, |\Delta \mathbf{A}| \leq \epsilon |\hat{\mathbf{L}}| |\hat{\mathbf{U}}|\} = \max_i \frac{|\mathbf{A} \hat{\tilde{\mathbf{u}}} - \mathbf{b}|_i}{(|\hat{\mathbf{L}}| |\hat{\mathbf{U}}| |\hat{\tilde{\mathbf{u}}}|)_i}, \quad (13)$$

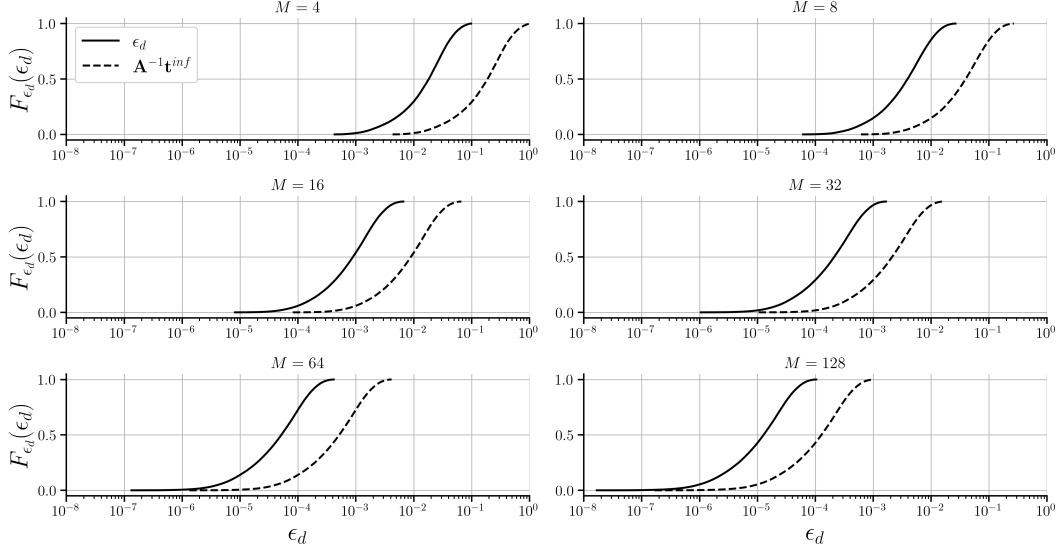


Figure 6: Empirical distribution function for true discretization error (—) and its bounds (---). To obtain the statistics, 10^4 independent experiments are conducted.

where $\hat{\mathbf{u}}$ is the finite-precision approximation to the solution of the linear system of equations [28, Theorem 7.3]. Using theorem 3.7, variance-informed backward error bounds for solving the tri-diagonal system

$$(\mathbf{A} + \Delta\mathbf{A})\hat{\mathbf{u}} = \mathbf{b}; \quad |\Delta\mathbf{A}| \leq \hat{\gamma}_{LS}|\hat{\mathbf{L}}||\hat{\mathbf{U}}|, \quad (14)$$

holds with a probability at least $\mathcal{Q}(\zeta, 7(M - 1) - 6)$.

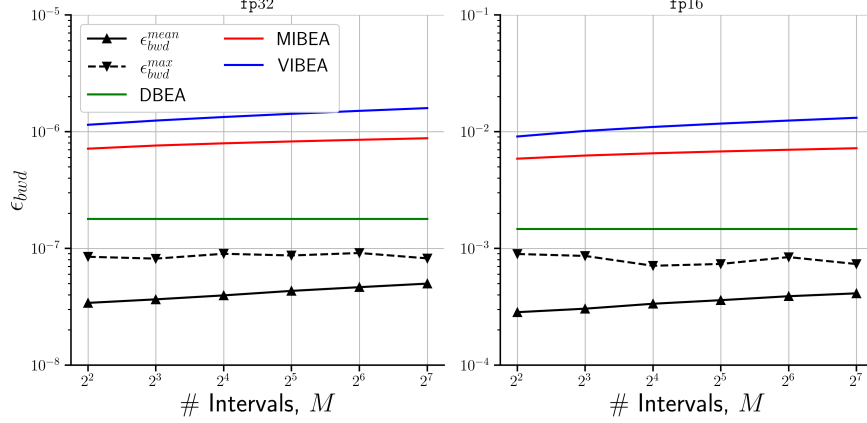


Figure 7: Backward error and its bounds for the solution of the ODE vs. number of discretization intervals M . To obtain the error bounds, we set $\mathcal{Q}(\zeta, 7(M - 1) - 6) = 0.99$. DBEA produces tighter estimates compared to MIBEA and VIBEA. To obtain the statistics, 10^5 independent experiments are conducted.

Figure 7 illustrate the backward error and its bounds for computing $\hat{\mathbf{u}}$ in **fp32** and **fp16**. With increasing discretization intervals M , the backward error increases marginally. For all M , the bounds obtained using the deterministic analysis result in a tighter estimate than the probabilistic approaches MIBEA and VIBEA, which overestimate the backward error by nearly an order of magnitude. This is expected for the Thomas algorithm due to the limited number of floating-point operations (at most two rounding errors per floating-point number), as shown in fig. 1. Further, since the number of arithmetic operations $n = 2 < n_c, n_d$, VIBEA-based bounds over-predict the backward error. Using Oettli-Prager theorem [28], the forward error bound is

$$\|\hat{\mathbf{u}} - \tilde{\mathbf{u}}\|_\infty \leq \hat{\gamma}_{LS}\mathcal{C}_{LS}; \quad \mathcal{C}_{LS} \triangleq \| |\mathbf{A}^{-1}| (|\hat{\mathbf{L}}||\hat{\mathbf{U}}||\hat{\mathbf{u}}|) \|_\infty, \quad (15)$$

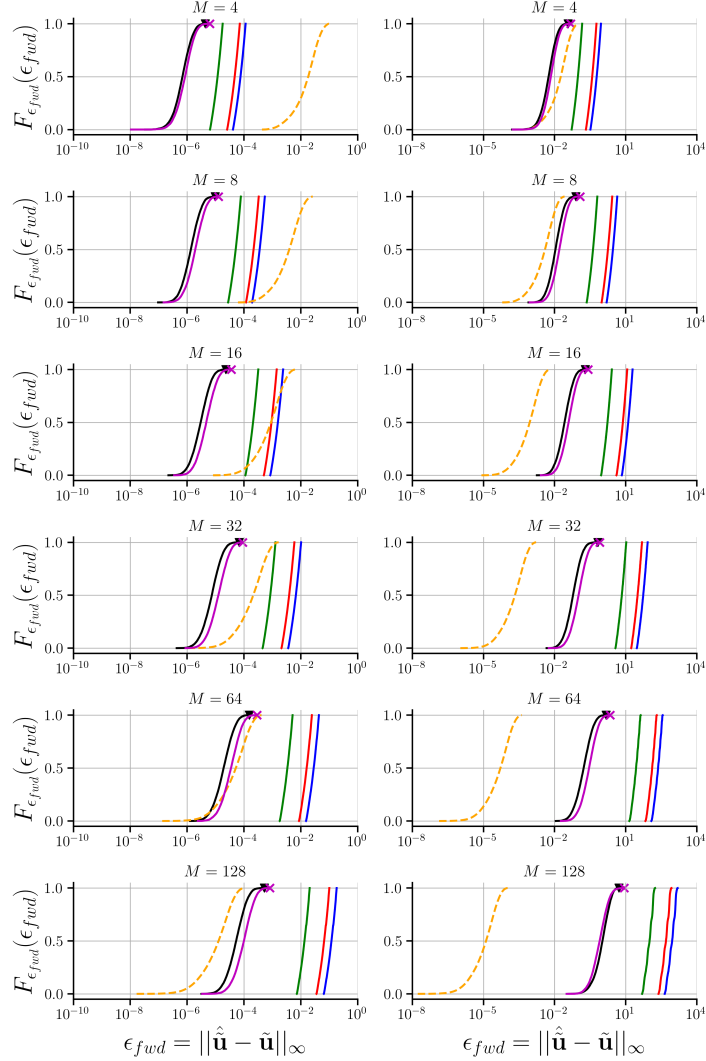


Figure 8: Empirical distribution function of the forward error (—) for computing $\hat{\mathbf{u}}$ in **fp32** (left column) and **fp16** (right column). To obtain the error bounds, we set $\mathcal{Q}(\zeta, 7(M-1)-6) = 0.99$. Error bounds obtained using DBEA (—) produce tighter estimates compared to MIBEA (—) and VIBEA (—) for all intervals M and precision. Largest true backward error (\blacktriangledown) is similar to the modeled backward error (\blacklozenge). To obtain the statistics, 10^4 independent experiments are conducted.

that holds with a probability of at least $\mathcal{Q}(\zeta, 7(M-1)-6)$. Figure 8 shows the EDF of the true forward error, modeled forward error (model 2.4), and the obtained forward error bounds for computations in **fp32** and **fp16** arithmetic. The modeled forward error approximates the true forward error for all discretization intervals and precision. Similar to fig. 7, the deterministic bounds estimate the forward error within an order of magnitude, and the probabilistic approaches produce pessimistic bounds. Further, the discretization error dominates over the rounding error for coarser discretization. With an increase in M , the total number of arithmetic operations increases and results in a larger rounding error, which dominates over the discretization error. For the computed solution $\hat{\mathbf{u}}$, theorem 3.1 can be used to obtain the backward error for the Riemann integration to obtain the finite-precision approximation $\hat{\tilde{p}}$ to \tilde{p}

$$\hat{\tilde{p}} = \sum_{i=1}^{M-1} (\hat{u}_i + \Delta \hat{u}_i) \Delta x_i; \quad |\Delta \hat{u}_i| \leq \hat{\gamma}_{M-1} |\hat{u}_i|,$$

that is satisfied with a probability of at least $\mathcal{Q}(\zeta, M-1)$. In the case of uniform grid spacing $\Delta x_i = \Delta x$. In addition to a rounding error when performing the Riemann summation, there exists a rounding error in computing $\hat{\mathbf{u}}$ as described by eq. (15). Thus, the forward error in computing $\hat{\mathbf{u}}$ can be propagated

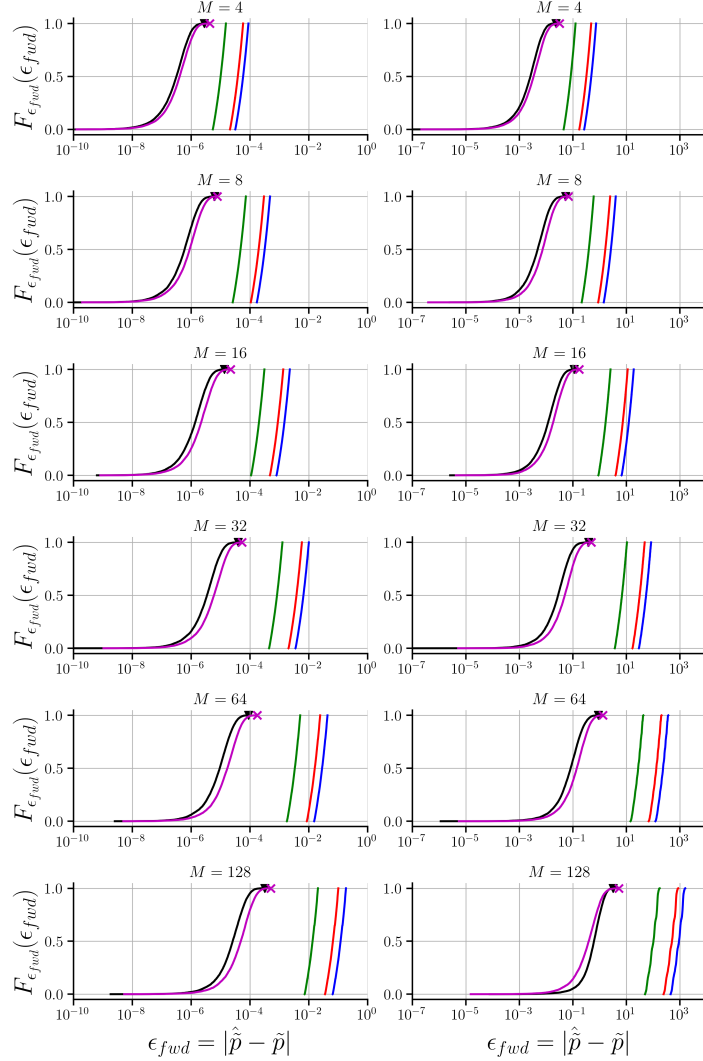


Figure 9: Empirical distribution function of the forward error (—) for computing \hat{p} in **fp32** (left column) and **fp16** (right column). We set $\mathcal{Q}(\zeta, 8M - 14) = 0.99$ to obtain the error bounds. Error bounds obtained using DBEA (—) produce tighter estimates compared to MIBEA (—) and VIBEA (—) for all intervals M and precision. Largest true backward error (✕) is similar to the modeled backward error (✕). To obtain the statistics, 10^4 independent experiments are conducted.

to obtain the absolute error in performing the Reimann integration as

$$\begin{aligned}
 |\hat{p} - \tilde{p}| &= \left| \sum_{i=1}^{M-1} (\hat{u}_i - \tilde{u}_i) \Delta x + \Delta \hat{u}_i \Delta x \right|, \\
 &\leq \sum_{i=1}^{M-1} |\hat{u}_i - \tilde{u}_i| |\Delta x| + |\Delta \hat{u}_i| |\Delta x|, \\
 &\leq \Delta x \left((M-1) \hat{\gamma}_{LS} \mathcal{C}_{LS} + \hat{\gamma}_{M-1} \|\hat{\mathbf{u}}\|_1 \right), \tag{16}
 \end{aligned}$$

that is satisfied with a probability of at least $1 - [(1 - \mathcal{Q}(\zeta, 7(M-1) - 6)) + (1 - \mathcal{Q}(\zeta, M-1))] = \mathcal{Q}(\zeta, 8M - 14)$. Figure 9 shows the EDF of the forward error, modeled forward error (model 2.4) and its bounds for computing \hat{p} in **fp32** and **fp16** arithmetic. The modeled forward error produces a good approximation to the true forward error. Similar to fig. 8, the deterministic bounds estimate the forward error within an order of magnitude, and the probabilistic approaches produce pessimistic bounds.

Figure 10 illustrates the absolute forward error in computing the quantity of interest $\mathbb{E}[P]$ using

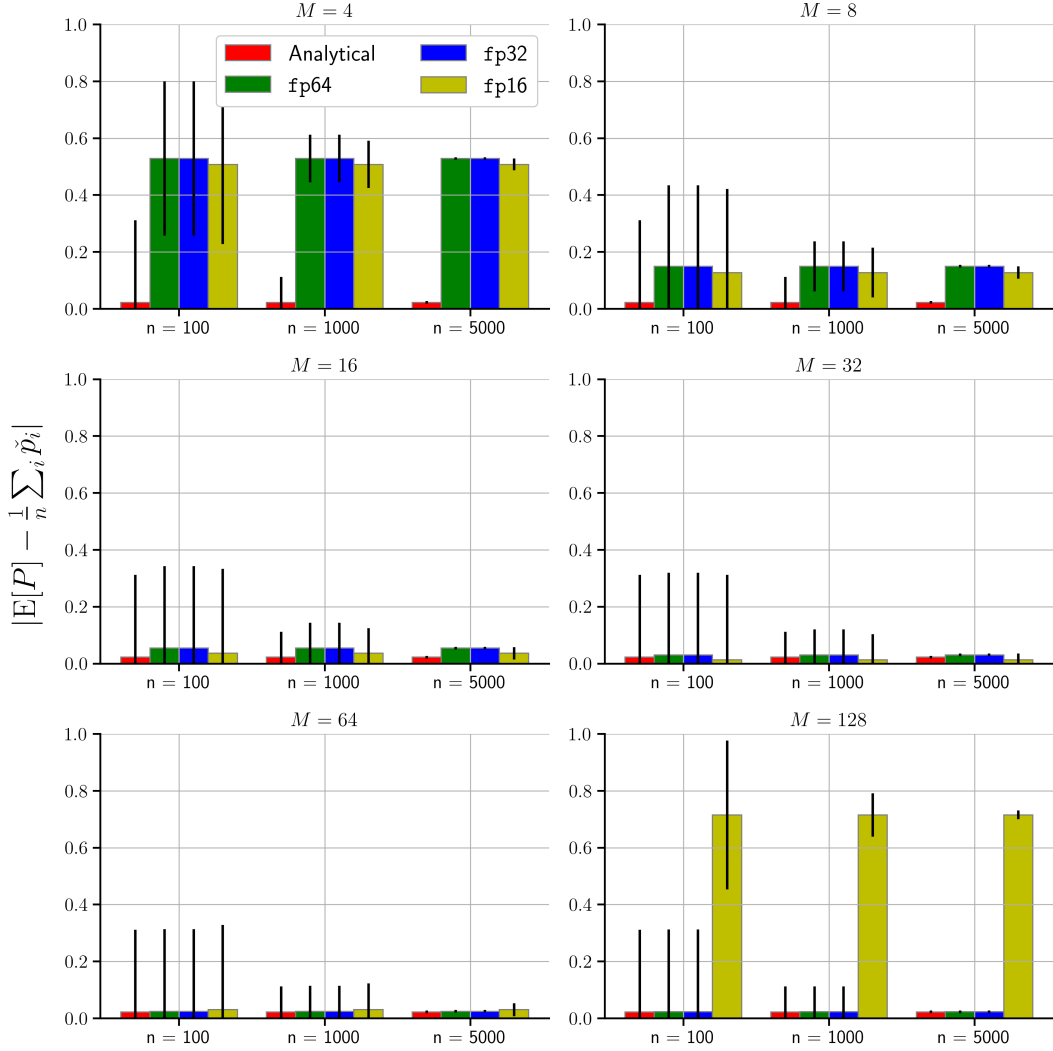


Figure 10: Absolute forward error in computing the quantity of interest $\mathbb{E}[P]$ using Monte-Carlo integration with n samples for varying discretization intervals M . Here $\tilde{p} = \tilde{p}$ for the analytical solution and $\hat{p} = \hat{p}$ for the finite-precision approximation.

Monte-Carlo integration with n samples for varying discretization intervals M . For coarser discretization, the error remains nearly consistent across all precision, indicating dominant uncertainty from numerical discretization compared to rounding or sampling. This error decreases with an increase in discretization intervals. Increasing the number of Monte-Carlo samples reduces the sampling uncertainty; however, for $M = \{2^i\}_{i=2}^6$, discretization error still dominates, and therefore, for such discretizations, we can leverage lower-precision arithmetic to accelerate computations. However, at $M = 128$, the accumulated rounding uncertainty is significantly higher than the discretization error, indicating that the increased computational efficiency from lower-precision arithmetic may be compromised by the increased uncertainty due to rounding. Thus, higher precision is required for reliable model prediction at finer discretizations.

5. Concluding remarks

In this work, we presented a novel variance-informed backward error analysis, called VIBEA, for quantifying the uncertainty due to rounding in floating-point computations. We leverage the IEEE arithmetic model without underflow and overflow and model the rounding errors as random variables. The proposed analysis only assumes that the rounding errors are bounded and are independent and identically distributed (i.i.d.), and it can leverage the rounding error statistics such as mean, variance,

and their bounds. Specifically, to bound the rounding errors, we leverage Bernstein’s concentration inequality, which can exploit higher-order statistics of random variables. We show that the \sqrt{n} dependence of the problem-size-dependent constant can be rigorously derived using the statistical description of rounding error without modeling assumptions about the functional form of the probabilistic bounds. Leveraging higher-order statistics, we propose a new problem-size-dependent constant $\hat{\gamma}_n$ that can be used to quantify the rounding uncertainty in the computed result for all problem size n . Following the proposed probabilistic analysis framework, we also demonstrate that the problem-size-dependent constant $\tilde{\gamma}_n \propto \lambda\sqrt{n}u$ proposed by Higham and Mary [1] can be improved by removing non-essential modeling assumptions. Specifically, we derive a closed-form expression for λ that depends on the bounds of the rounding error distribution and the required confidence in the bounds.

We present a special case of VIBEA, where a non-informative rounding error distribution $\mathcal{U}[-u, u]$ is considered. This distribution marginally overestimates the accumulated rounding error and provides a good approximation of the maximum accumulated rounding error. We demonstrate that, compared to previous work by Higham and Mary [1] and the widely used deterministic rounding error analysis, the proposed problem-size-dependent constant $\hat{\gamma}_n$ scales well with the number of arithmetic operations and can provide much tighter estimates for low-precision arithmetic. Nearly $\mathcal{O}(10^6)$ improvement can be obtained by VIBEA for low-precision arithmetic compared to previous work.

Numerical experiments are presented for dot products and matrix-vector multiplication using random data and a stochastic boundary value problem that utilizes the Thomas algorithm. We demonstrate that for $n \geq 4$, VIBEA can provide tighter bounds compared to the analysis presented by Higham and Mary [1] with very high confidence. We demonstrate that nearly an order of magnitude improvement can be obtained for dot products and matrix-vector multiplication. However, in the regime of small arithmetic operations per floating-point value, as observed in the case of the stochastic boundary value problem, the probabilistic approach (both VIBEA and the analysis presented by Higham and Mary [1]) produces pessimistic bounds compared to the deterministic approach.

We demonstrate that to leverage low-precision arithmetic for statistical models with different sources of uncertainties, it is paramount that rounding uncertainty should be quantified alongside other sources to ensure gain in computational efficiency does not sacrifice accuracy. In the stochastic boundary value problem, we show that for coarser discretization, the error due to numerical discretization is dominant compared to the uncertainty due to rounding or sampling. In such a regime, low-precision arithmetic can be reliably used to gain computational efficiency. However, at finer discretization levels, the rounding uncertainty at low precision can be orders of magnitude larger. Thus, carefully selecting precision is required to obtain model predictions with a desirable accuracy.

This work highlights the need to understand the different uncertainties in floating-point statistical models for more nuanced optimization strategies, such as balancing numerical discretization with evaluation precision or obtaining the requisite parameter samples to address sampling uncertainty. The insights from such a comprehensive uncertainty budgeting are crucial for strategically allocating computational efforts, enabling the development of reliable and cost-efficient models.

Reproducibility of computational results

Code for the experiments performed is available at <https://github.com/sahilbhola14/FinUQ>.

Acknowledgments

This work is dedicated to the memory of the late Prof. Nick Higham whose work continues to inspire the field of numerical analysis. We thank Profs. Jean-Baptiste Jeannin and Alex Gorodetsky for advice and for the valuable feedback on the early drafts of this manuscript. This research was supported by NSF Grant FMITF-2219997.

References

- [1] N. J. Higham, T. Mary, A new approach to probabilistic rounding error analysis, *SIAM journal on scientific computing* 41 (5) (2019) A2815–A2835.
- [2] S. Gupta, A. Agrawal, K. Gopalakrishnan, P. Narayanan, Deep learning with limited numerical precision, in: *International conference on machine learning*, PMLR, 2015, pp. 1737–1746.

- [3] N. Wang, J. Choi, D. Brand, C.-Y. Chen, K. Gopalakrishnan, Training deep neural networks with 8-bit floating point numbers, *Advances in neural information processing systems* 31 (2018).
- [4] I. Hubara, M. Courbariaux, D. Soudry, R. El-Yaniv, Y. Bengio, Quantized neural networks: Training neural networks with low precision weights and activations, *Journal of Machine Learning Research* 18 (187) (2018) 1–30.
- [5] E. A. Paxton, M. Chantry, M. Klöwer, L. Saffin, T. Palmer, Climate modeling in low precision: Effects of both deterministic and stochastic rounding, *Journal of Climate* 35 (4) (2022) 1215–1229.
- [6] T. Kimpson, E. A. Paxton, M. Chantry, T. Palmer, Climate-change modelling at reduced floating-point precision with stochastic rounding, *Quarterly Journal of the Royal Meteorological Society* 149 (752) (2023) 843–855.
- [7] S. Hatfield, M. Chantry, P. Düben, T. Palmer, Accelerating high-resolution weather models with deep-learning hardware, in: *Proceedings of the platform for advanced scientific computing conference*, 2019, pp. 1–11.
- [8] N. J. Higham, S. Pranesh, M. Zounon, Squeezing a matrix into half precision, with an application to solving linear systems, *SIAM journal on scientific computing* 41 (4) (2019) A2536–A2551.
- [9] A. Haidar, H. Bayraktar, S. Tomov, J. Dongarra, N. J. Higham, Mixed-precision iterative refinement using tensor cores on gpus to accelerate solution of linear systems, *Proceedings of the Royal Society A* 476 (2243) (2020) 20200110.
- [10] A. Haidar, P. Wu, S. Tomov, J. Dongarra, Investigating half precision arithmetic to accelerate dense linear system solvers, in: *Proceedings of the 8th workshop on latest advances in scalable algorithms for large-scale systems*, 2017, pp. 1–8.
- [11] A. Abdelfattah, H. Anzt, E. G. Boman, E. Carson, T. Cojean, J. Dongarra, A. Fox, M. Gates, N. J. Higham, X. S. Li, et al., A survey of numerical linear algebra methods utilizing mixed-precision arithmetic, *The International Journal of High Performance Computing Applications* 35 (4) (2021) 344–369.
- [12] A. Buttari, J. Dongarra, J. Langou, J. Langou, P. Luszczek, J. Kurzak, Mixed precision iterative refinement techniques for the solution of dense linear systems, *The International Journal of High Performance Computing Applications* 21 (4) (2007) 457–466.
- [13] Y. Liu, X. Liu, E. Wu, Real-time 3d fluid simulation on gpu with complex obstacles, in: *12th Pacific Conference on Computer Graphics and Applications*, 2004. PG 2004. *Proceedings.*, IEEE, 2004, pp. 247–256.
- [14] P. R. Rinaldi, E. Dari, M. J. Vénere, A. Clause, A lattice-boltzmann solver for 3d fluid simulation on gpu, *Simulation Modelling Practice and Theory* 25 (2012) 163–171.
- [15] M. Karp, F. Liu, R. Stanly, S. Rezaeiravesh, N. Jansson, P. Schlatter, S. Markidis, Uncertainty quantification of reduced-precision time series in turbulent channel flow, in: *Proceedings of the SC’23 Workshops of The International Conference on High Performance Computing, Network, Storage, and Analysis*, 2023, pp. 387–390.
- [16] G. Lienhart, A. Kugel, R. Manner, Using floating-point arithmetic on fpgas to accelerate scientific n-body simulations, in: *Proceedings. 10th Annual IEEE Symposium on Field-Programmable Custom Computing Machines*, IEEE, 2002, pp. 182–191.
- [17] M. Baboulin, A. Buttari, J. Dongarra, J. Kurzak, J. Langou, J. Langou, P. Luszczek, S. Tomov, Accelerating scientific computations with mixed precision algorithms, *Computer Physics Communications* 180 (12) (2009) 2526–2533.
- [18] S. Mittal, A survey of techniques for approximate computing, *ACM Computing Surveys (CSUR)* 48 (4) (2016) 1–33.
- [19] N. J. Higham, S. Pranesh, Simulating low precision floating-point arithmetic, mims eprint 2019.4, Manchester Institute for Mathematical Sciences, The University of Manchester, UK (2019).

- [20] B. Feng, Y. Wang, G. Chen, W. Zhang, Y. Xie, Y. Ding, Egemm-tc: accelerating scientific computing on tensor cores with extended precision, in: Proceedings of the 26th ACM SIGPLAN symposium on principles and practice of parallel programming, 2021, pp. 278–291.
- [21] J. Richard Shewchuk, Adaptive precision floating-point arithmetic and fast robust geometric predicates, *Discrete & Computational Geometry* 18 (1997) 305–363.
- [22] NVIDIA Blackwell architecture, <https://resources.nvidia.com/en-us-blackwell-architecture>.
- [23] C. J. Roy, W. L. Oberkampf, A comprehensive framework for verification, validation, and uncertainty quantification in scientific computing, *Computer methods in applied mechanics and engineering* 200 (25-28) (2011) 2131–2144.
- [24] S. Wan, R. C. Sinclair, P. V. Coveney, Uncertainty quantification in classical molecular dynamics, *Philosophical Transactions of the Royal Society A* 379 (2197) (2021) 20200082.
- [25] A. Cherezov, A. Vasiliev, H. Ferroukhi, Acceleration of nuclear reactor simulation and uncertainty quantification using low-precision arithmetic, *Applied Sciences* 13 (2) (2023) 896.
- [26] N. J. Higham, How accurate is gaussian elimination?, Tech. rep., Cornell University (1989).
- [27] N. J. Higham, Bounding the error in gaussian elimination for tridiagonal systems, *SIAM journal on matrix analysis and applications* 11 (4) (1990) 521–530.
- [28] N. J. Higham, Accuracy and stability of numerical algorithms, SIAM, 2002.
- [29] D. Mori, Y. Yamamoto, S.-L. Zhang, Backward error analysis of the allreduce algorithm for householder qr decomposition, *Japan journal of industrial and applied mathematics* 29 (2012) 111–130.
- [30] A. E. Kellison, A. W. Appel, M. Tekriwal, D. Bindel, Laproof: A library of formal proofs of accuracy and correctness for linear algebra programs, in: Proceedings of the 30th IEEE International Symposium on Computer Arithmetic (ARITH)(Sept. 2023). <https://github.com/ak-2485/ak-2485.github.io/blob/master/laproof.pdf>, 2023.
- [31] A. Buttari, N. J. Higham, T. Mary, B. Vieublé, A modular framework for the backward error analysis of gmres (2024).
- [32] J. Von Neumann, H. H. Goldstine, Numerical inverting of matrices of high order (1947).
- [33] T. E. Hull, J. R. Swenson, Tests of probabilistic models for propagation of roundoff errors, *Communications of the ACM* 9 (2) (1966) 108–113.
- [34] P. Henrici, Test of probabilistic models for the propagation of roundoff errors, *Communications of the ACM* 9 (6) (1966) 409–410.
- [35] M. Tienari, A statistical model of roundoff error for varying length floating-point arithmetic, *BIT Numerical Mathematics* 10 (3) (1970) 355–365.
- [36] I. C. Ipsen, H. Zhou, Probabilistic error analysis for inner products, *SIAM journal on matrix analysis and applications* 41 (4) (2020) 1726–1741.
- [37] J. H. Wilkinson, Error analysis of direct methods of matrix inversion, *Journal of the ACM (JACM)* 8 (3) (1961) 281–330.
- [38] J. H. Wilkinson, Rounding errors in algebraic processes, SIAM, 2023.
- [39] N. J. Higham, T. Mary, Sharper probabilistic backward error analysis for basic linear algebra kernels with random data, *SIAM Journal on Scientific Computing* 42 (5) (2020) A3427–A3446.
- [40] M. P. Connolly, N. J. Higham, Probabilistic rounding error analysis of householder qr factorization, *SIAM Journal on Matrix Analysis and Applications* 44 (3) (2023) 1146–1163.

- [41] IEEE, Ieee standard for floating-point arithmetic, ieee std 754-2019 (revision of ieee 754-2008), Institute of Electrical and Electronics Engineers New York, 2019.
- [42] M. Croci, M. Fasi, N. J. Higham, T. Mary, M. Mikaitis, Stochastic rounding: implementation, error analysis and applications, Royal Society Open Science 9 (3) (2022) 211631.
- [43] S. Boucheron, G. Lugosi, O. Bousquet, Concentration inequalities, in: Summer school on machine learning, Springer, 2003, pp. 208–240.
- [44] W. Oettli, W. Prager, Compatibility of approximate solution of linear equations with given error bounds for coefficients and right-hand sides, Numerische Mathematik 6 (1964) 405–409.
- [45] M. B. Giles, Multilevel monte carlo methods, Acta numerica 24 (2015) 259–328.

Appendix A. Rounding errors in floating point arithmetic

The floating-point number system $\mathbb{F} \subset \mathbb{R}$ consists of numbers with the form

$$y \triangleq \pm d_0.d_1d_2 \cdots d_{p-1} \times \beta^e,$$

where p is the *precision*, β is the *base*, and $e \in [e_{min}, e_{max}]$ is the *exponent*. Here, $0 \leq d_i \leq \beta - 1$ and $d_0 \neq 0$ for normalized numbers. Given the tuple $t^* \triangleq (p, \beta, e_{min}, e_{max})$, a finite and unique set of representable numbers can be obtained that defines a floating-point system. Representing $z \in \mathbb{R}$ in a floating-point number system characterized by t^* thus requires a projection operation $fl : \mathbb{R} \rightarrow \mathbb{F}$ such that $fl(z) \in \mathbb{F}$ is a representable number. This projection operation to a representable number is called *representation-rounding*. A similar rounding operation occurs when finite-precision arithmetic operations are performed. For $a, b \in \mathbb{F}$, computing $(a \text{ op } b)$ where $op \in \{+, -, \times, /\}$ in the prescribed precision requires a projection to a representable number $fl(a \text{ op } b) \in \mathbb{F}$. This projection operation associated with finite-precision arithmetic is called *operation-rounding*. The loss of information due to representation- or operation-rounding introduces rounding errors that grow during successive computations, thus introducing rounding uncertainty in the computational model. As a result, computing any function $\varphi : \mathbb{R}^{n_{in}} \rightarrow \mathbb{R}^{n_{out}}$ in finite precision produces an approximation $\hat{\mathbf{y}}$ of $\mathbf{y} = \varphi(\mathbf{x})$, which is the true output of an approximate function $\hat{\varphi}$ as illustrated in fig. A.11. To measure the quality of approximation $\hat{\mathbf{y}}$, *forward errors* can be defined, which are the absolute or relative errors described in the output space [28]. Since the true output \mathbf{y} is typically unknown, forward error bounds can be developed (a process called forward error analysis) to estimate the uncertainty introduced due to rounding. Alternatively, the uncertainty introduced due to rounding can be interpreted as a consequence of perturbations in the input space that propagates through the true function φ [28]. To this end, an input perturbation $\Delta \mathbf{x}$ can be defined to find the set of inputs that solves the actual problem, that is, $\varphi(\mathbf{x} + \Delta \mathbf{x}) = \hat{\varphi}(\mathbf{x})$. Since $\Delta \mathbf{x}$ can be non-unique, the smallest relative perturbation to the input space called the *backward error* can be defined. This can be obtained as the solution to an optimization problem

$$\epsilon_{bwd} \triangleq \min\{\epsilon \geq 0 : \hat{\mathbf{y}} = \varphi(\mathbf{x} + \Delta \mathbf{x}), |\Delta \mathbf{x}| \leq \epsilon |\mathbf{x}|\}.$$

Appendix B. Model for Rounding Error Distribution

Figure B.12 illustrates the empirical distribution function (EDF) for the true and modeled (model 2.4) rounding error for the addition and multiplication operation using data sampled randomly from $\mathcal{U}[2^k, 2^{k+1}]$. Specifically, we select $k = 0$ and $k = 7$ to avoid overflow for both addition and multiplication operations in `fp32` and `fp16`. For a random variables X , the EDF is defined as $F_X(t) \triangleq \frac{1}{n} \sum_{i=1}^n \mathbf{1}_{X=x_i \leq t} \in [0, 1]$, where x_i denotes an observation of the random variable X and $\mathbf{1}$ is an indicator function. Thus, if $F_{X_1}(t) < F_{X_2}(t)$, where X_1 and X_2 are random variables defined on the same support would mean that there is a *smaller probability* that X_1 is less than t compared to X_2 . For $z \in \mathcal{U}[2^k, 2^{k+1}] \forall k \in \mathbb{I}$, where \mathbb{I} denotes the set of integers, a similar EDF is obtained as a consequence of uniform spacing between representable numbers within the interval $[\beta^k, \beta^{k+1}]$, where β is the base [28]. As observed, the modeled rounding error results in a larger rounding error with higher

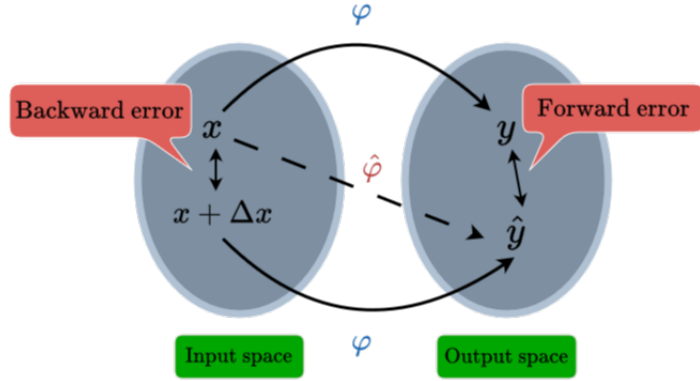


Figure A.11: Schematic of backward and forward errors. Solid line (—): exact; dashed line (---): computed.

probability and, therefore, overestimates the true rounding error on average. This overestimation is desirable as any rounding error bounds developed using model 2.4 must not bound under-predicted accumulated rounding errors. However, model 2.4 is not always realistic. For example, model 2.4 results in a zero-mean rounding error distribution, which becomes invalid when adding large positive numbers to very small positive numbers [1]. Nevertheless, the motivation for using model 2.4 is to obtain reasonable estimates for rounding uncertainty on average.

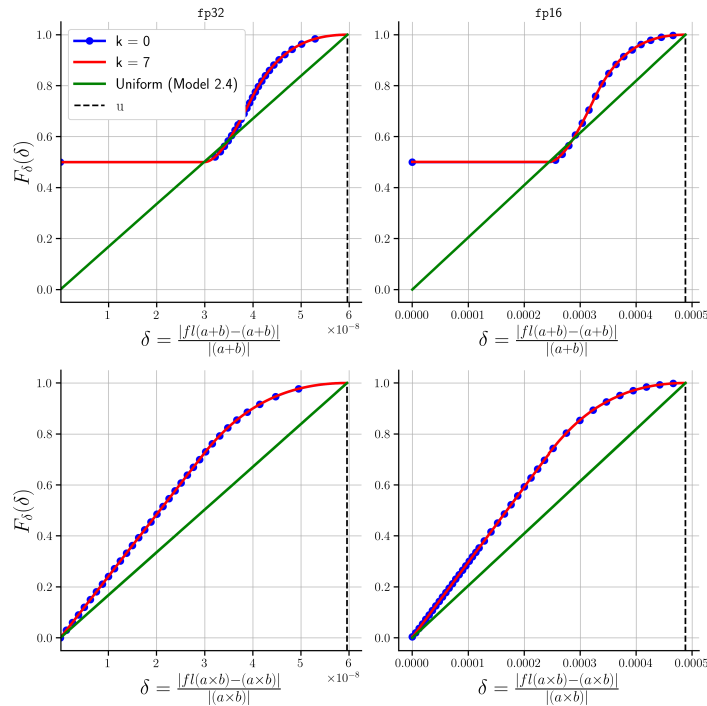


Figure B.12: Empirical distribution function of the true and modeled (model 2.4) absolute relative error for addition (top row) and multiplication (bottom row) operation using random data sampled as $\mathcal{U}[2^k, 2^{k+1}]$. Double-precision `fp64` arithmetic is considered as the exact result. Markers are skipped for visualization purposes.